

## Recent progress and prospects of Li-CO<sub>2</sub> batteries: Mechanisms, catalysts and electrolytes

Yanan Jiao<sup>a</sup>, Jian Qin<sup>b,c,\*</sup>, Hirbod Maleki Kheimeh Sari<sup>b,c</sup>, Dejun Li<sup>a</sup>, Xifei Li<sup>a,b,c,\*</sup>, Xueliang Sun<sup>a,b,c,d,\*</sup>

<sup>a</sup> Tianjin International Joint Research Centre of Surface Technology for Energy Storage Materials, College of Physics and Materials Science, Tianjin Normal University, Tianjin 300387, China

<sup>b</sup> Xi'an Key Laboratory of New Energy Materials and Devices, Institute of Advanced Electrochemical Energy & School of Materials Science and Engineering, Xi'an University of Technology, Xi'an 710048, China

<sup>c</sup> Xi'an Key Laboratory of New Energy Materials and Devices, Xi'an, Shaanxi, 710048, China

<sup>d</sup> Department of Mechanical and Materials Engineering, University of Western Ontario, London, ON N6A 5B9, Canada

### ARTICLE INFO

**Keywords:**  
Li-CO<sub>2</sub> battery  
Reaction mechanism  
Cathode catalyst  
Electrolyte

### ABSTRACT

Combining balanced CO<sub>2</sub> emissions with energy storage technologies is an effective way to alleviate global warming caused by CO<sub>2</sub> emissions and meet the growing demand for energy supplies. Li-CO<sub>2</sub> electrochemical system has attracted much attention due to its promising energy storage and CO<sub>2</sub> capture strategy. However, the system is still in the early stages of development and faces huge challenges because of the many problems caused by the slow kinetics of the CO<sub>2</sub> electrochemical reaction. In this review, along with introducing the charge-discharge reaction mechanism of Li-CO<sub>2</sub> battery, the latest development of the battery's cathode electrode material and electrolyte composition and its impact on electrochemical performance are systematically addressed. A comprehensive understanding of Li-CO<sub>2</sub> batteries is intended to provide useful guidance for the development of high-performance and practical advanced Li-CO<sub>2</sub> batteries.

### 1. Introduction

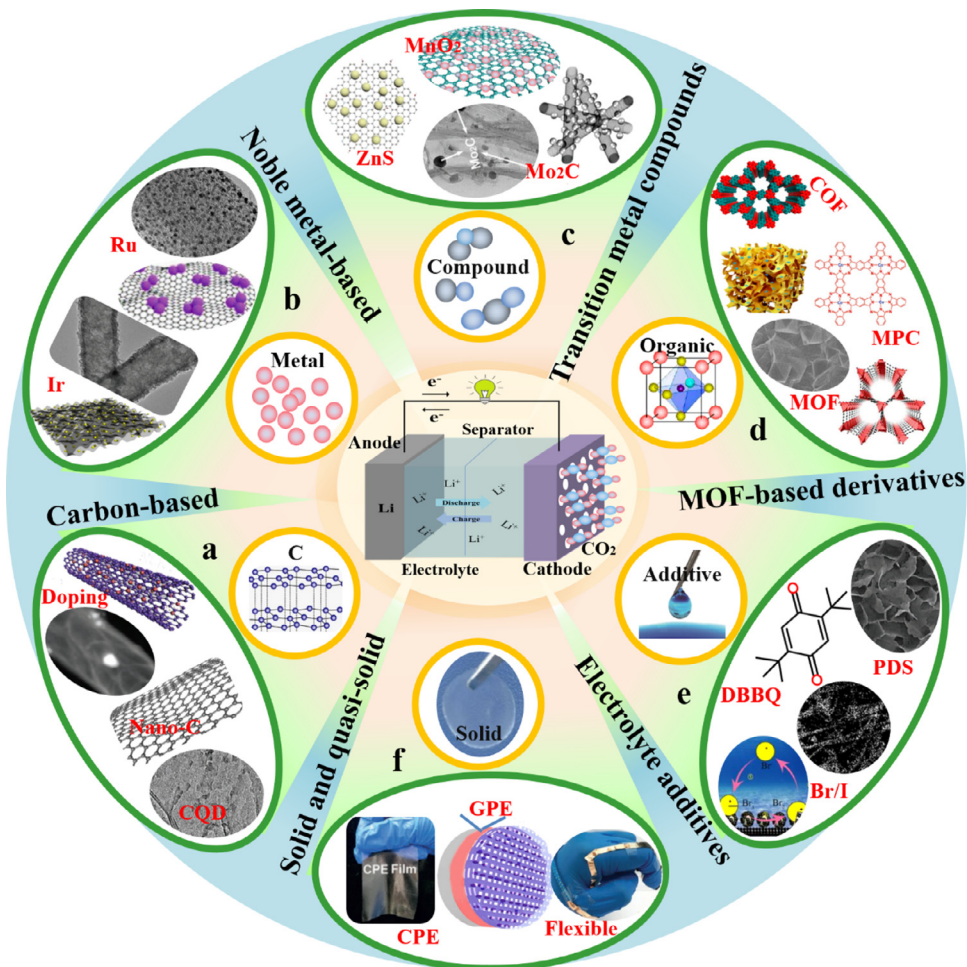
In today's society, with the rapid growth of economy and technology, people's demand for more energy supplies progressively increases, resulting in excessive consumption of non-renewable fossil fuels, which not only caused an energy crisis, but also caused the continuous emission of greenhouse gases (mainly CO<sub>2</sub>), accelerating global warming [1–6]. Therefore, solving these problems is a great challenge for achieving a sustainable social development [7]. In recent years, scientists have worked on developing renewable energy sources that enable energy conversion and storage, such as secondary batteries [8–10], supercapacitors [11–13] and fuel cells, [14–16] which may partially replace fossil fuels.

Since its commercialization in 1991, lithium-ion batteries (LIBs) have dominated the portable electronic market and changed our lives; [17] however, its limited specific energy density cannot meet the high energy density demand of electric vehicles and large-scale grid energy storage [18–22]. Therefore, it is necessary to find an energy equipment with higher specific energy density. Many researchers have turned their attention to metal-air batteries [23–47]. Particularly for lithium-air (Li-air) batteries, the theoretical specific energy density is as high as 3500 Wh kg<sup>-1</sup>, which has attracted more attention from scientists [48–53]. It

is well known that Li-air batteries have an open system, and this structure obtains and transfers electric energy through a conversion reaction of oxygen in the atmosphere. Despite the promising future, the development of Li-air batteries is still plagued by many problems. It is worth noting that most Li-air batteries are lithium-oxygen (Li-O<sub>2</sub>) batteries [54–60], which usually work with pure oxygen rather than air, and are therefore susceptible to air pollution, such as carbon dioxide (CO<sub>2</sub>) and water (H<sub>2</sub>O) [61]. In a humid environment, moisture in the air can degrade battery performance due to the following chemical reactions between H<sub>2</sub>O and Li<sub>2</sub>O<sub>2</sub> (the main discharge product of the battery): 2Li<sub>2</sub>O<sub>2</sub> + 2H<sub>2</sub>O = 4LiOH + O<sub>2</sub> [62–64]. In addition, CO<sub>2</sub> in the air is easily soluble in organic solvents. Solvated CO<sub>2</sub> is extremely easy to react with superoxide radicals in the air and form Li<sub>2</sub>CO<sub>3</sub> at the cathode. Under the influence of CO<sub>2</sub>, there will be continuous driving force to convert Li<sub>2</sub>O<sub>2</sub> to Li<sub>2</sub>CO<sub>3</sub> [65,66]. However, the stability of Li<sub>2</sub>CO<sub>3</sub> is higher than that of Li<sub>2</sub>O<sub>2</sub>. The high decomposition potential of Li<sub>2</sub>CO<sub>3</sub> reduces the reversibility and cycle life of the battery [61,67]. Therefore, scientists began to find solutions for the harmful effects of CO<sub>2</sub> on Li-air batteries. In 2011, Takechi et al. reported Li-O<sub>2</sub>/CO<sub>2</sub> batteries for the first time [68], and found that the introduction of CO<sub>2</sub> increases the discharge capacity to a great extent. Subsequent studies shifted their

\* Corresponding authors.

E-mail addresses: [qinjian@xaut.edu.cn](mailto:qinjian@xaut.edu.cn) (J. Qin), [xli2011@hotmail.com](mailto:xli2011@hotmail.com) (X. Li), [xsun9@uwo.ca](mailto:xsun9@uwo.ca) (X. Sun).



focus to CO<sub>2</sub> by creating a battery system with CO<sub>2</sub> as the working gas [69,70]. The birth of lithium carbon dioxide (Li-CO<sub>2</sub>) batteries can be described as killing two birds with one stone by using greenhouse gases as energy source, which not only reduces the accumulation of CO<sub>2</sub>, but also provides power for energy conversion and storage [71–77].

Despite the many benefits of Li-CO<sub>2</sub> batteries, this area of research is still in its infancy. Typically, Li-CO<sub>2</sub> batteries are composed of Li metal anodes, organic/solid-state electrolytes, ionic conductive separators and porous cathodes (including additives, adhesives, catalysts, etc.) [75,78,79]. The battery participates in the absorption and release of CO<sub>2</sub> gas through charging and discharging. It is susceptible to several pitfalls: (1) there is a large overpotential between the reduction reaction and the CO<sub>2</sub> precipitation reaction; (2) the generated wide band gap in Li<sub>2</sub>CO<sub>3</sub> is difficult to decompose; (3) the generated C deposits on the cathode surface. These three issues are often attributed to several factors, including complex multiple interface reactions, slow reaction kinetics of carbonate products, lack of effective catalysts, volatilization and decomposition of electrolytes, and corrosion of metallic lithium cathodes. Therefore, researchers have made great efforts to solve these problems and improve the electrochemical performance of Li-CO<sub>2</sub> batteries.

Herein, to manifestly elaborate the latest progress about Li-CO<sub>2</sub> electrochemistry, the electrochemical reaction mechanism of Li-CO<sub>2</sub> batteries is firstly discussed. More importantly, recent advances in cathode catalyst and electrolyte design are addressed (Fig. 1). Moreover, some controversies and challenges of Li-CO<sub>2</sub> batteries are reviewed. It is believed that this review may be beneficial of understanding Li-CO<sub>2</sub> batteries systems to design practical batteries in the future.

**Fig. 1.** Schematic illustration of catalyst and electrolyte species in Li-CO<sub>2</sub> batteries.

## 2. Electrochemical reaction mechanism of Li-CO<sub>2</sub> batteries

Although the history of Li-CO<sub>2</sub> batteries inspired by Li-O<sub>2</sub> batteries is relatively short, its electrochemical mechanism has made a great progress in less than a decade. It is well known that the Li-CO<sub>2</sub> electrochemical reaction is very complex, involving multiple interface reactions between CO<sub>2</sub> gas, electrolyte, catalyst and reaction products. Elucidating the basic reaction mechanism of Li-CO<sub>2</sub> batteries is the basis for understanding the system and selecting suitable electrolyte and catalyst. In this section, the charging and discharging mechanism of the system is fully explained by the discharge products of Li-CO<sub>2</sub> batteries (Li<sub>2</sub>CO<sub>3</sub>, C, Li<sub>2</sub>O, CO, Li<sub>2</sub>C<sub>2</sub>O<sub>4</sub>, etc.).

### 2.1. $\text{CO}_2 \leftrightarrow \text{Li}_2\text{CO}_3 + \text{C}$

In 2013, Archer et al. made the first primary Li-CO<sub>2</sub> battery using pure CO<sub>2</sub> as a working gas [75], and the ectopic Fourier transform infrared spectra (FTIR) and X-ray diffraction (XRD) were used to fully prove that the main component of the discharge product is Li<sub>2</sub>CO<sub>3</sub>. It involved a feasible electrochemical reactions such as Eq. (1).



In the following year, Chen's group [80] verified this idea using Ketjen Black (KB) as the cathode catalyst and lithium triflate (LiCF<sub>3</sub>SO<sub>3</sub>) in TEGDME (1: 4 in mole) as the electrolyte. Encouragingly, at room temperature, the reversible discharge specific capacity reached about 1032 mAh g<sup>-1</sup> based on the weight of KB. Experiments have shown that specific electrolytes can result in CO<sub>2</sub> reduction reactions. They

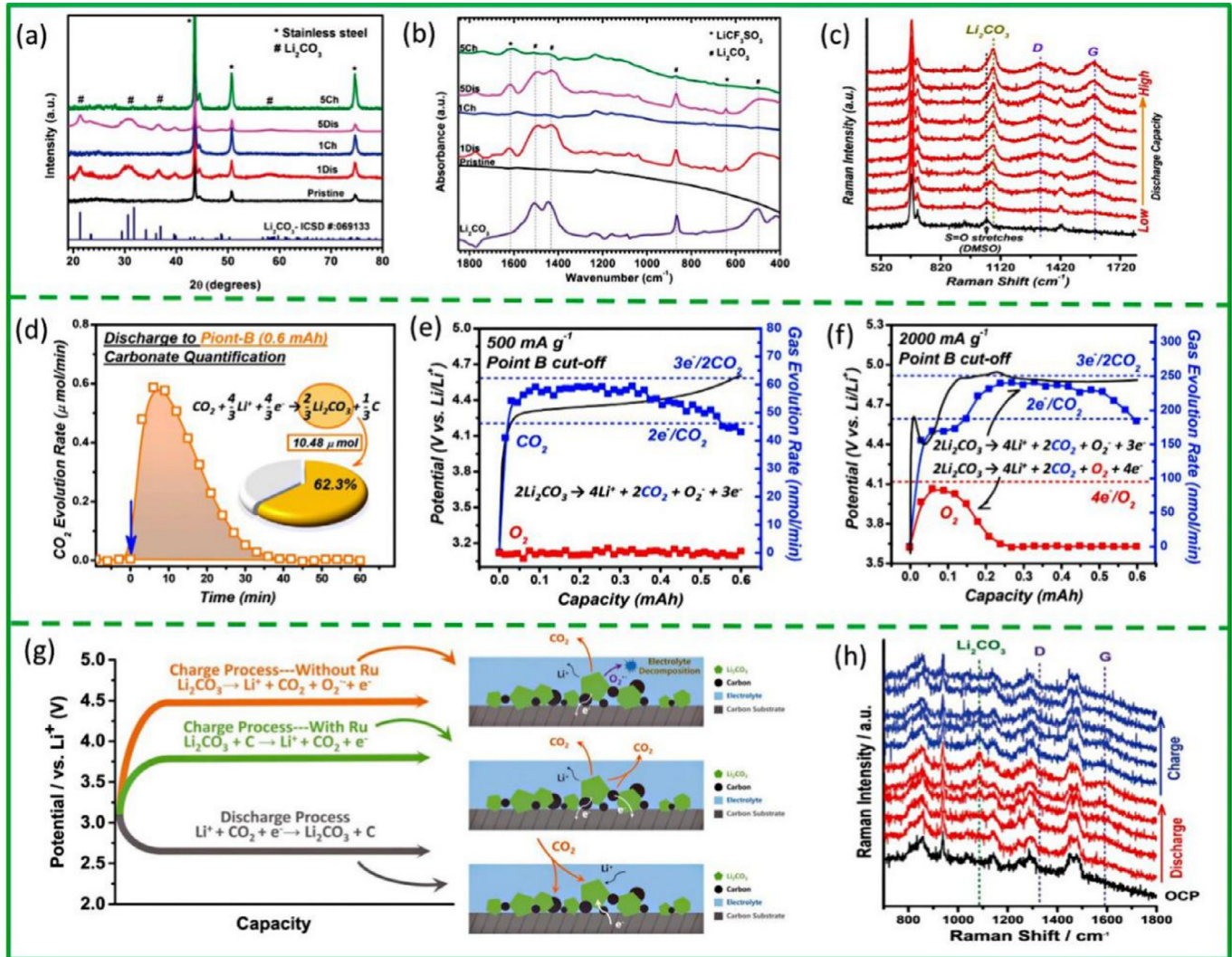
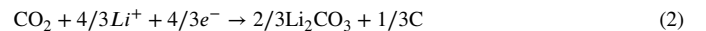


**Fig. 2.** (a) XRD pattern of the original KB electrode in Li-CO<sub>2</sub> batteries. (b) FTIR spectra [80]. (c) Raman spectrum. (d) CO<sub>2</sub> evolution rate during carbonate quantification. The DEMS result of the gas escape rate of CO<sub>2</sub> and O<sub>2</sub> during batteries charging: (e) 500 mA g<sup>-1</sup>, and (f) The current density after discharge to point B is 2000 mA g<sup>-1</sup> [83]. (g) Schematic diagram of Li-CO<sub>2</sub> batteries during charging and discharging. (h) Schematic representation of in-situ SERS characterization [90].

confirmed the formation and decomposition of Li<sub>2</sub>CO<sub>3</sub> using XRD and FTIR. As shown in Fig. 2a, the XRD pattern shows that Li<sub>2</sub>CO<sub>3</sub> is the main discharge product after the first and fifth discharge and it can also be decomposed at high voltage, indicating a reversible process. The similar results can also be seen in the FTIR spectrum through the appearance and disappearance of the vibration modes around 868 cm<sup>-1</sup>, 1431 cm<sup>-1</sup> and 1505 cm<sup>-1</sup> (see Fig. 2b). In addition, Surface Enhanced Raman Spectroscopy (SERS) and Electron Energy Loss Spectroscopy (EELS) were employed to further investigate the discharge product, and amorphous C was observed by using porous gold as the reference instead. Although the reaction mechanism thermodynamic and kinetic properties in Li-CO<sub>2</sub> batteries with porous Au and KB as cathode are similar, it still needs more studies. Subsequently, many researchers have confirmed the formation and decomposition of Li<sub>2</sub>CO<sub>3</sub> and C [81,82] with advanced technologies, such as in-situ differential electrochemical mass spectroscopy (DEMS), X-ray photoelectron spectroscopy (XPS), in-situ gas chromatography-mass spectrometry (GC-MS), etc.

Based on a carbon cathode, GC-MS is used [83]. During the discharging process, by monitoring the release rate of CO<sub>2</sub> gas after acid treatment on the discharged cathode (Fig. 2d), the corresponding quantification of carbonates shows that 10.48 mmol of Li<sub>2</sub>CO<sub>3</sub> has formed (B

Point: 0.6 mAh capacity). Compared with the theoretical amount of reduced CO<sub>2</sub> species calculated from the discharge capacity, the yield of fixed Li<sub>2</sub>CO<sub>3</sub> (62.3%) indicates that the discharge reaction can be accurately defined as Eq. (2).



However, the discharging reaction path of Li-CO<sub>2</sub> batteries is still unclear. Therefore, based on the discharging products (Li<sub>2</sub>CO<sub>3</sub> and C) and the proven disproportionation of LiO<sub>2</sub> in Li-O<sub>2</sub> batteries [84–87], Chen and his colleagues [88] reasonably assumed that certain disproportionation reactions need to be placed in Li-CO<sub>2</sub> batteries, involving the reaction Eqs. (3)–(6).



**Table 1**

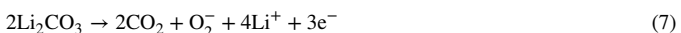
Possible reactions of  $\text{Li}_2\text{CO}_3$  decomposition and Gibbs free energy and the reversible potential of corresponding reactions [89].

No.	Possible Reactions	$E_{\text{rev}}/\text{V}_{\text{vs.Li}}$
1	$\text{Li}_2\text{CO}_3 \rightarrow \text{CO}_2 + 1/2\text{O}_2 + 2\text{Li}^+ + 2\text{e}^-$	3.82
2	$\text{Li}_2\text{CO}_3 + 1/2\text{C} \rightarrow 2\text{Li}^+ + 3/2\text{CO}_2 + 2\text{e}^-$	2.80
3	$\text{Li}_2\text{CO}_3 \rightarrow \text{CO}_2 + 2\text{Li}^+ + \text{O}_2^-$ $\text{O}_2^- \rightarrow \text{O}_2$ $\text{O}_2^- + \text{O}_2 + \text{electrolyte} \rightarrow \text{uncertain product}$	Unknown Value

[Eq. \(3\)](#) shows the single electron reduction of  $\text{CO}_2$  on the surface of a carbon material to  $\text{C}_2\text{O}_4^{2-}$ . [Eqs. \(4\)](#) and [\(5\)](#) may indicate that the unstable  $\text{C}_2\text{O}_4^{2-}$  is decomposed into  $\text{CO}_3^{2-}$  and C in two steps. In [Eq. \(6\)](#),  $\text{Li}_2\text{CO}_3$  was formed in crystals. Immediately after, Zhou research group [83] used in-situ SERS technology to study the discharge mechanism of Li-CO<sub>2</sub> batteries on the gold cathode. The experimental results were almost similar to the Chen group's assumptions. Based on the corresponding in-situ Raman spectra recorded during the discharge ([Fig. 2c](#)), the specific vibration mode in  $\text{Li}_2\text{CO}_3$  and the D/G band in C can be clearly observed.

Although this discharge process is widely accepted, the charging mechanism is very vague. Zhou's group [89] focused on the reaction mechanism of electrochemical decomposition of  $\text{Li}_2\text{CO}_3$  in an aprotic electrolyte environment. They used in-situ GC-MS measurement and isotopic tracing method to detect the gas components generated during the charging process of the pre-filled electrode, and confirmed that  $\text{Li}_2\text{CO}_3$  was decomposed into  $\text{CO}_2$ , superoxide radicals and dissolved oxygen. Indeed, the assumptions about possible reaction paths are presented in [Table 1](#).

Afterwards, by using DEMS, the corresponding gas escape rate was studied at various current rates [83]. At a relatively low charge rate (500 mA g<sup>-1</sup>, [Fig. 2e](#)), no  $\text{O}_2$  can be detected and only  $\text{CO}_2$  release can be observed. The relevant  $\text{CO}_2$  mass-to-charge ratio (close to  $3\text{e}^-/2\text{CO}_2$ ) indicates that the charging process can be regarded as a separate decomposition of  $\text{Li}_2\text{CO}_3$ , and the relevant process can be depicted as [Eq. \(7\)](#). However, at higher current rates (2000 mA g<sup>-1</sup>, [Fig. 2f](#)), the release of  $\text{CO}_2$  and  $\text{O}_2$  can be observed in the initial stage of charging, and the mass-to-charge ratios are  $2\text{e}^-/\text{CO}_2$  and  $4\text{e}^-/\text{O}_2$ . Therefore, the decomposition reaction of  $\text{Li}_2\text{CO}_3$  can be defined as [Eq. \(8\)](#).



This study only involved the decomposition process of  $\text{Li}_2\text{CO}_3$ , and it did not mention the reversible decomposition of C material. Subsequently, Zhou's group used  $\text{Li}_2\text{CO}_3$ -C electrodes to simulate the cathode of discharged Li-CO<sub>2</sub> batteries [90]. The decomposition of C was achieved through technical improvement ([Fig. 2g](#)). As shown in [Fig. 2h](#), the peak intensity (1580 cm<sup>-1</sup>) of the G band in C shows a decrease during charging and completely disappears at the end of charging process. In-situ SERS and GC-MS results show that the common reaction of  $\text{Li}_2\text{CO}_3$  and C is achieved during the charging process, [Eq. \(9\)](#), rather than the self-decomposition of  $\text{Li}_2\text{CO}_3$ .



Li-CO<sub>2</sub> batteries are commonly recognized as four electrons reaction [90–92]. Through a series of characterization techniques, such as DEMS and Raman spectroscopy, the reversible decomposition of crystalline  $\text{Li}_2\text{CO}_3$  and amorphous C was confirmed, and carbon neutrality was maintained [93]. Thus, reversible Li-CO<sub>2</sub> batteries were obtained, according to the reaction process shown in [Eq. \(10\)](#).



However, the specific reaction mechanism is still very controversial. This reversible process requires a charging voltage higher than 4 V, which can easily cause many side reactions. It is known that an effective and strong catalyst can reduce the overvoltage during charging and realize effective Li-CO<sub>2</sub> batteries, as described below.

## 2.2. $\text{CO}_2 \leftrightarrow \text{Li}_2\text{C}_2\text{O}_4$

In the previous studies,  $\text{Li}_2\text{C}_2\text{O}_4$  has been investigated as an intermediate discharge product in non-aqueous Li-CO<sub>2</sub> batteries [83,94]. However, some studies have found that the presence of Mo<sub>2</sub>C can stabilize this intermediate product [88,95]. In these batteries, the Mo<sub>2</sub>C catalyst can stably generate  $\text{C}_2\text{O}_4^{2-}$ , preventing it from further reaction to form carbonates and C ([Fig. 3a](#)), reducing the charging voltage, making reversible reactions easier to occur, and realizing reversible Li-CO<sub>2</sub> batteries. The discharge process of the battery can be described as [Eq. \(11\)](#).



Chen and colleague's work [88] showed that after discharge an amorphous  $\text{Li}_2\text{C}_2\text{O}_4$ -Mo<sub>2</sub>C is generated, which is more susceptible to decomposition than  $\text{Li}_2\text{CO}_3$ . Indeed, the reaction kinetics is accelerated, the voltage platform is reduced, and the charging reaction is more likely to occur. The reaction steps can be summarized as [Eqs. \(12\)](#) and [\(13\)](#).



Subsequently, DFT calculation confirms [95] that the delocalized electrons generated by the low-valent Mo atoms through the Mo-O coupling bridge in Mo<sub>2</sub>C can stabilize the amorphous intermediate discharge product  $\text{Li}_2\text{C}_2\text{O}_4$  ([Fig. 3b](#)). The thermodynamically unstable  $\text{Li}_2\text{C}_2\text{O}_4$  is easier to decompose, and the decomposition process is described as [Eq. \(14\)](#).



## 2.3. $\text{CO}_2 \leftrightarrow \text{CO}$

In this field of electrochemical CO<sub>2</sub> reduction research, many commercial chemicals can be indirectly produced by converting CO<sub>2</sub> to CO and then further reducing it. It is believed that direct synthesis of CO can only be accomplished through inexpensive or low-selectivity catalysts, which makes CO an important industrial raw material [96]. Therefore, the Li-CO<sub>2</sub> battery system that generates CO gas becomes a substantial medium for using valuable chemicals and fuels in the future.

Archer's group [75] assumed that the simplest known reaction between Li and CO<sub>2</sub> dominates the discharge process, as shown in [Eq. \(15\)](#):



However, when the discharge temperature is 100 °C, the theoretical equilibrium potential for CO generation is 2.5 V by thermodynamic calculation, which is lower than the actual charging potential of 2.65 V. According to Tafel's theory, the actual discharge potential cannot exceed the theoretical equilibrium potential, which indicates that the proposed reaction is likely to be only partially correct. Recently, Wang's group [97] solved this problem. They used TEGDME electrolyte and 3D porous fractal zinc (PF-Zn) cathode material to realize Li-CO<sub>2</sub> batteries that can generate CO gas instead of amorphous C species. They identified the presence of CO products via gas chromatography (GC). The Li-CO<sub>2</sub> battery produces a CO content of 3.6% at 0.01 mA, and its Faradic efficiency (FE) at 0.1 mA gradually increases to a maximum of 67%. When the applied current is further increased, the CO produced

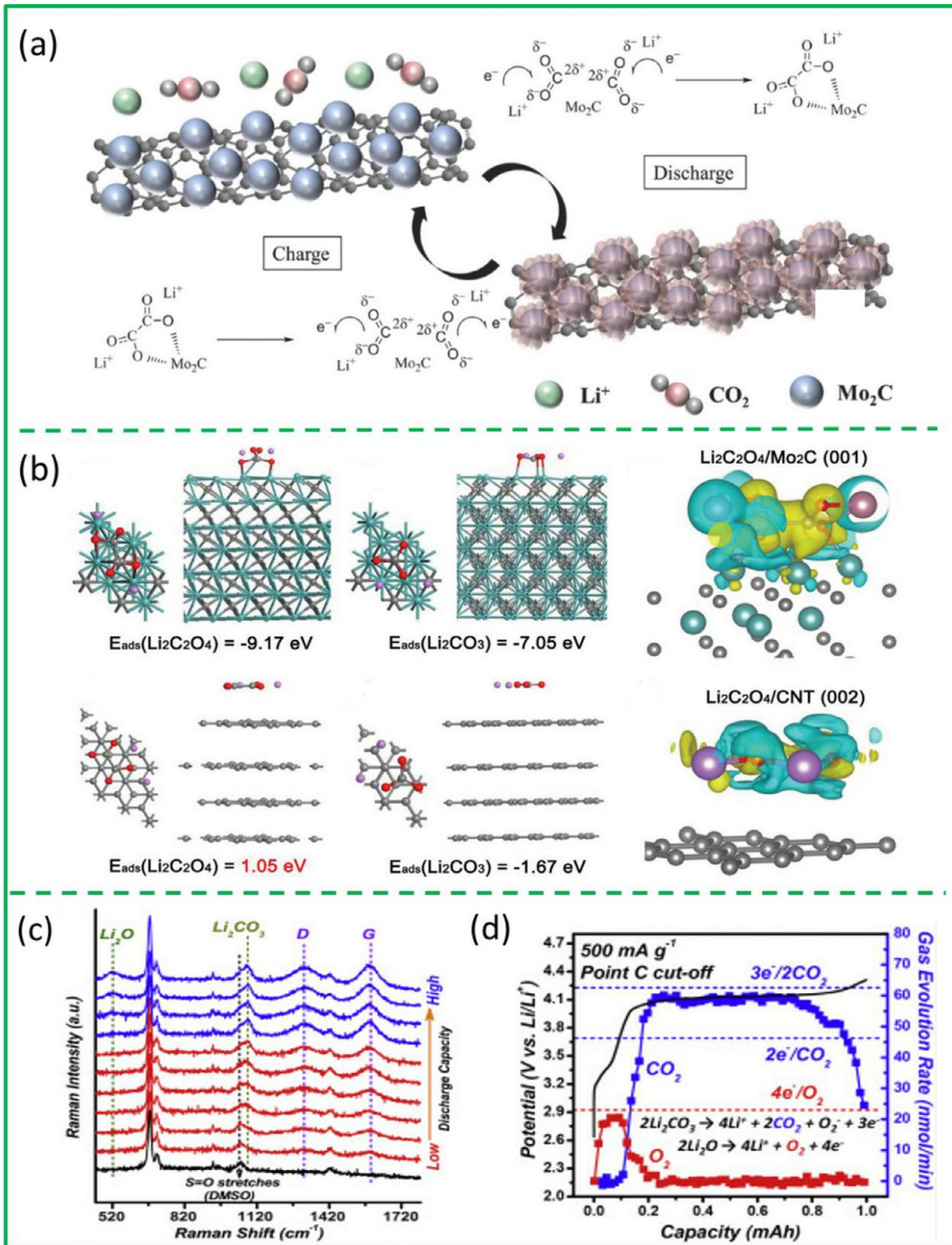


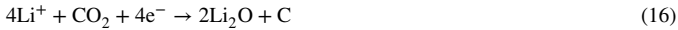
**Fig. 3.** (a) Schematic of the reactions during the discharge and charging of  $\text{Mo}_2\text{C}/\text{CNT}$  in  $\text{Li}-\text{CO}_2$  batteries [88]. (b) Top view of the most energy-optimized structure with optimized energy [95]. (c) In-situ Raman spectrum. (d) CO FE during long-term discharge of 0.1 mA [83].

by the  $\text{Li}-\text{CO}_2$  batteries has a lower FE, which may be attributed to the further expanded overpotential and the coverage of the solid product on the cathode surface. This work demonstrates the feasibility of exploring high-value carbon-based commodities from  $\text{Li}-\text{CO}_2$  batteries systems. However, more research is required to combine power generation technology with the production of carbon-based value-added chemicals and fuels.

#### 2.4. $\text{CO}_2 \leftrightarrow \text{Li}_2\text{O} + \text{C}$

Usually the reaction of  $\text{Li}_2\text{CO}_3$  generation is at 2.5 V. Surprisingly, Zhou et al. [83] found a plateau at a lower voltage (1.8 V). Observing the in-situ Raman spectrum (Fig. 3c), it was found that a new peak gradually appeared at  $520 \text{ cm}^{-1}$ , which may be attributed to  $\text{Li}_2\text{O}$ . Combined with the first-principles calculation results, Eq. (16) is used to illustrate the

new discharge plateau.



In the subsequent stage of the initial charge at a lower potential, O<sub>2</sub> release was observed (Fig. 3d). In addition, based on the 4e<sup>-</sup>/O<sub>2</sub> mass-to-charge ratio obtained at the corresponding stage, the elemental decomposition pathway of the obtained Li<sub>2</sub>O can be further determined as in Eq. (17).



In a nutshell, Li-CO<sub>2</sub> electrochemical reaction is affected by many factors, including temperature, humidity, current density, discharge depth, working gas composition, catalyst, electrolyte composition, etc. Therefore, the detailed reaction path is still controversial and needs more research. However, with the advent of advanced characterization tools and in-situ analysis techniques, it is believed that the basic mechanism will be perceived in the near future. In the following sections, the effects of catalysts and electrolytes on Li-CO<sub>2</sub> batteries are explained.

### 3. Cathode catalyst of Li-CO<sub>2</sub> batteries

Cathode catalysts play a significant role in promoting the electrochemical reaction kinetics to reduce the overpotential between charge and discharge, thereby playing a key role in achieving feasible and reversible Li-CO<sub>2</sub> batteries. Compared with Li-O<sub>2</sub> batteries, Li-CO<sub>2</sub> batteries have higher requirements on catalysts. Li-CO<sub>2</sub> battery catalysts need to have better catalytic ability to reduce the reaction overpotential. It requires a larger active area to provide more catalytic active centers, and it also needs to avoid C deposition, so as to make the chemical reaction more reversible. Therefore, the development of catalysts with high catalytic activity and conductivity is crucial to the research of high-performance Li-CO<sub>2</sub> batteries. In the past few years, researchers have conducted extensive research on various catalysts, including carbon-based, precious metal-based, transition metal compound-based, and macromolecular compound catalysts. In this section, we systematically explain the latest progress and design strategies of various catalysts based on the type of catalytic material, and the overall impact of the chemical composition and spatial structure of catalysts on CO<sub>2</sub> reduction and release in Li-CO<sub>2</sub> batteries. Then, the challenges and future development opportunities for an effective catalyst design are discussed.

#### 3.1. Carbon-based catalyst

Carbonaceous materials have the advantages of high conductivity, large specific surface area, light weight, and adjustable surface activity sites. They can be used as conductive agents, electrode materials and catalytic carriers, and have been widely used in various fields of electrochemistry, and recently, as cathode catalysts in Li-CO<sub>2</sub> batteries. Moreover, commercial C materials, such as KB or conductive carbon black (Super P), have also attracted much attention due to excellent electronic conductivity, large surface area and commercial availability [68,75,80]. Takechi et al. found that based on a KB cathode, employing ester electrolytes can only yield a small capacity (66 mAh g<sup>-1</sup>) [68]. However, the combination of KB cathode and ether electrolyte in Li-CO<sub>2</sub> batteries can deliver a discharge capacity exceeding 1000 mAh g<sup>-1</sup>, and work for 7 cycles at a current density of 30 mA g<sup>-1</sup> [80]. Compared with KB cathodes, Super P cathodes exhibit lower discharge capacity in ionic liquid-based electrolytes [75], while a discharge capacity of 6062 mAh g<sup>-1</sup> can be obtained in ether electrolytes and maintain for nearly 20 cycles at a current density of 100 mA g<sup>-1</sup> [90]. The above studies have found that commercial C materials can be used as cathode catalysts under the premise of using the appropriate electrolyte. Unfortunately, the inherent spatial structure and restricted CO<sub>2</sub> catalytic activity of commercial C materials limit the battery performance. Therefore, these C materials are not ideal catalysts for Li-CO<sub>2</sub> batteries.

Nano-carbon materials exhibit better physical and chemical properties than commercial C materials. Carbon nanotube (CNT) is a member of the nano-carbon family, and a one-dimensional quantum material with high conductivity and porous structure. Because of its high conductivity and porous structure, it has been considered as a promising candidate for Li-CO<sub>2</sub> batteries cathode materials. In 2015, Zhou et al. introduced CNT into Li-CO<sub>2</sub> batteries for the first time [98]. These batteries with CNT cathode can provide an initial discharge capacity of 8379 mAh g<sup>-1</sup> at a current density of 50 mA g<sup>-1</sup>, and work stably in 20 cycles at 100 mA g<sup>-1</sup> while the cut-off capacity is 1000 mAh g<sup>-1</sup>. However, because Li<sub>2</sub>CO<sub>3</sub> with wide band gap is difficult to decompose, the overpotential during charging is still very high (4.5 V), which greatly limits the practical application of Li-CO<sub>2</sub> batteries. Graphene is another member of the nano-carbon family. It is a two-dimensional nanomaterial composed of carbon atoms and sp<sup>2</sup> hybrid orbital hexagonal honeycomb lattice, which has high electrochemical stability and high specific surface area. Zhou et al. in another pioneering work introduced graphene into Li-CO<sub>2</sub> batteries as cathode [81], which delivered high discharge capacities of up to 14774 and 7000 mAh g<sup>-1</sup> with stable cyclabilities over 20 and 10 cycles at current densities of 50 and 100 mA g<sup>-1</sup>, respectively. Although graphene cathodes have satisfactory electrochemical activity and cycle capacity in Li-CO<sub>2</sub> batteries, great improvements must be done about their kinetic parameters to achieve high-efficiency catalysts. Guo and Wang et al. used pencil drawings on C paper as cathode catalysts [99], as shown in Fig. 4a-e. The pencil traces show a typical two-dimensional nanosheet structure, which is consist of finite-layer graphite. The stand-alone handwriting electrode exhibited a better cycle performance than the above-mentioned C materials, and maintained 45 cycles at a fixed discharge capacity of 1000 mAh g<sup>-1</sup> and a current density of 200 mA g<sup>-1</sup> (Fig. 4f).

In fact, defects are inevitable for C materials (i.e., pore structure, doped heteroatoms, edge defects, etc.) while also improve their electrochemical activity. Xing's group used a variety of C materials with different pore structures as cathode catalysts for Li-CO<sub>2</sub> batteries to reveal the effect of pore type on catalytic performance [100]. It was found that the shape, pore size and surface area of the pores are the key factors affecting their catalytic performance. The shape of the holes is the main influencing factor among these three factors. Two-dimensional and three-dimensional mesopores are better than ink bottle and one-dimensional mesopores. A large pore size is essential for maintaining a large reaction interface, and it is also beneficial to resist the blocking of pores by discharge products. These findings have important implications for the further development of high-performance carbon cathode catalysts in Li-CO<sub>2</sub> batteries.

Meanwhile, many researchers have turned their attention to heteroatom-doped carbon materials [101–105], including anionic doping, cation doping, and co-doping of heteroatoms, which can adjust the electronic structure, change the electronic properties of catalytic materials, and form more active sites. Nitrogen-doped carbon is a material with ultra-high specific surface area [106–110]. Doping pyridine nitrogen is an effective strategy to improve carbon-based catalysts for CO<sub>2</sub> reduction reaction (CO<sub>2</sub>RR) and evolution reaction (CO<sub>2</sub>ER).. Wang's group reported a highly surface-wrinkled and N-doped CNT network as a cathode catalyst [111]. The addition of N (3.68 wt%) caused a large number of voids and defects on the surface of CNT, thereby releasing more CO<sub>2</sub>RR and CO<sub>2</sub>ER active atoms (Fig. 5a-c). The adsorption energy value of Li on CNT and N-CNT shows that N doping can enhance the ability of capturing Li atoms by CNTs (Fig. 5e), and Li atoms are probably more stable in the N-6 induced defect center after doping (Fig. 5d). N-6 atom plays an important role in accelerating the diffusion of Li and CO<sub>2</sub> to the active catalytic sites and promoting the kinetics of CO<sub>2</sub> fixation reaction (Fig. 5f-g). A series of characterization and DFT studies have shown that Li<sub>2</sub>CO<sub>3</sub> can be reversibly deposited and decomposed on the fold wall of N-CNT. When evaluated as the positive electrode of Li-CO<sub>2</sub> batteries, it can provide a high discharge capacity of 9292.3 mAh g<sup>-1</sup> (Fig. 5h), improved cycle performance of 45 cycles along with

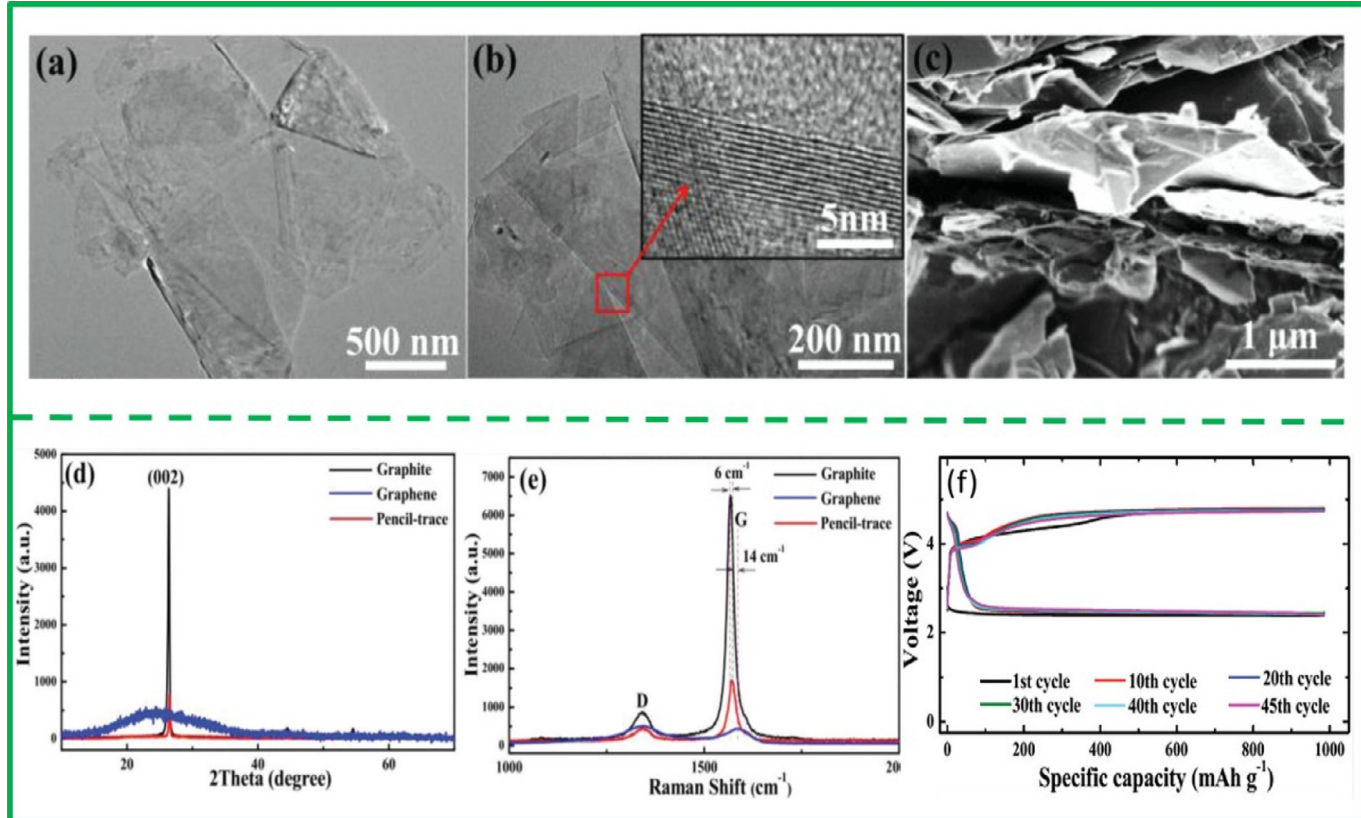


**Fig. 4.** (a,b,c) TEM and SEM images of pencil traces. (d) XRD pattern. (e) Raman spectra. (f) Cyclic performance of Li-CO<sub>2</sub> batteries using pencil traces without bonding electrodes at a current of 200 mA g<sup>-1</sup> and a fixed capacity of 1000 mAh g<sup>-1</sup> [99].

a good rate performance (Fig. 5i). Accordingly, the team also used the floating catalyst chemical vapor deposition (FCCVD) method to produce bamboo-like N-doped CNT fibers (B-NCNT) as a metal-free catalyst [77]. This B-NCNT material is rich in doped N, with a weight percentage up to 8.93 wt%. The pentagonal (N-5) and hexagonal (N-6) nitrogen centers produced by high N doping have higher electronic conductivity. In particular, N-6 doping has a direct positive effect on promoting the kinetics process. It is responsible for enhancing the CO<sub>2</sub>RR and CO<sub>2</sub>ER activity in this B-NCNT cathode. The fabricated Li-CO<sub>2</sub> batteries show good electrochemical performance with superior full discharge capacity of 23328 mAh g<sup>-1</sup>, high rate capability with a low potential gap up to 1.96 V at a current density of 1000 mA g<sup>-1</sup>, stability over 360 cycles, and satisfactory flexibility.

In addition to single atom doping studies, polyatomic doping has also attracted much attention. Dai et al. reported a new B, N-doped porous graphene (BN-hG) as an efficient dual-function cathode catalyst for rechargeable Li-CO<sub>2</sub> batteries [112]. Doping B and N dopants in graphene sheets can increase their electrical conductivity, which is beneficial for electron transport in the electrochemical process. The calculated B and N contents in the BN-hG were 2.6 and 4.1 at%, respectively. The initial discharge capacity was as high as 16033 mAh g<sup>-1</sup>, which is about 2.4 times that of hG cathode. The reversible charging capacity was 14996 mAh g<sup>-1</sup>, with the initial coulombic efficiency of 93.5%. At the same time, Li-CO<sub>2</sub> batteries with BN-hG cathodes showed a decent cycle stability at a high current density of 1.0 A g<sup>-1</sup> (i.e., 200 cycles), with an almost constant end-of-discharge voltage of 2.34 V. However, for the same batteries with hG cathodes, after the first 30 cycles, the end-of-discharge voltage quickly dropped to 2.0 V. Doping heteroatoms in the C skeleton introduces an uneven charge distribution and positively charges nearby C atoms, which is beneficial for the CO<sub>2</sub>RR and CO<sub>2</sub>ER.

Metal cation-doped C materials which promote CO<sub>2</sub> reduction have also attracted a lot of attention. Qiao et al. demonstrated that high load-

ing (about 5.3%) of single Co atom on graphene oxide (adjacent Co/GO) can serve as an efficient and durable electrocatalyst for Li-CO<sub>2</sub> batteries [113]. Experimental and theoretical simulations show that adjacent Co/GO has a unique electronic structure and a synergistic effect of Co-Co and Co-O binding. This targeted dispersion of Co atoms provides catalytically adjacent active sites, thereby achieving strong adsorption and reversible decomposition of Li<sub>2</sub>CO<sub>3</sub> discharge products. Adjacent Co/GO showed a very high sustained discharge capacity of 17358 mAh g<sup>-1</sup> at a current density of 100 mA g<sup>-1</sup> over 100 cycles.

It has been previously demonstrated that N-doped and metal ion-doped C materials can improve the CO<sub>2</sub> reduction and release activity to varying degrees. Heterogeneous co-doped C materials can not only provide more active sites, but also produce anion-cation synergistic catalysis. He et al. reported a Co-N-doped CNT (Co-N-CNT) material for Li-CO<sub>2</sub> cathode catalyst [74]. The Co and N contents in the CNT were 0.42 at% and 2.54 at%, respectively. The Co-N-CNT cathode showed lower polarization during charge/discharge. Co atoms are considered to be important for enhancing the catalytic activity of Li<sub>2</sub>CO<sub>3</sub> decomposition and CO<sub>2</sub> release. This Li-CO<sub>2</sub> battery displayed a high capacity of 6042 mAh g<sup>-1</sup> at a current density of 200 mA g<sup>-1</sup> and sustained good performance for 92 cycles at a high current density of 400 mA g<sup>-1</sup>. Indeed, as a comparison, N-CNT shows inferior reversibility and larger overpotential. Heteroatom-doped materials are more effective in activation of carbon atoms, which triggers more defects and reaction sites, and improves the catalytic activity of Li-CO<sub>2</sub> batteries.

Heteroatom-doped C materials can improve the catalytic activity of carbon-based cathodes, but the overpotential is still high at high current densities, which limits the practical development of Li-CO<sub>2</sub> batteries. Carbon quantum dots (CQD) have attracted widespread attention as effective electrochemical catalysts with effective edge defects and quantum confinement. However, the electrocatalytic activity of CQD is severely limited due to the poor conductivity of the original CQD.

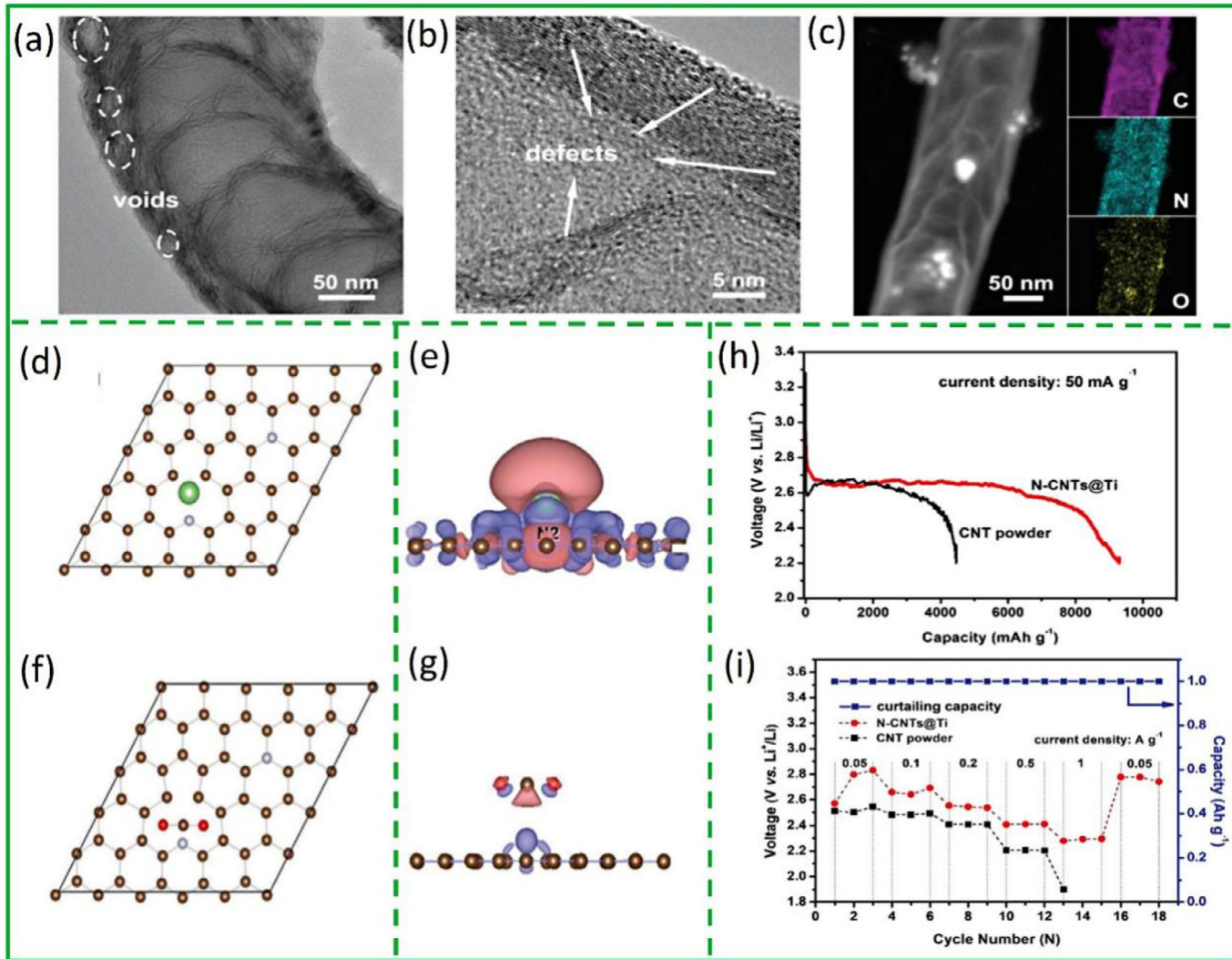


**Fig. 5.** (a,b) HRTEM images of N-doped CNTs (c) STEM image and corresponding element mappings. Top view of the optimized energetically most favorable structures of (d) Li, and (f) CO<sub>2</sub> adsorbed on N-6 site of pyridinic and graphitic N-doped CNT (002) surface. The brown, grey, green, and red balls represent C, N, Li, and O, respectively. Charge density difference of (e) Li and (g) CO<sub>2</sub> adsorbed on N-6 site of pyridinic and graphitic N-doped CNT (002) surface, respectively. The blue and pink regions represent the charge accumulation and charge loss, respectively. (h) Galvanostatic discharge/charge profiles of N-CNTs@Ti and CNT powder under CO<sub>2</sub> at a current density of 50 mA g<sup>-1</sup>. (i) Rate capabilities of the Li-CO<sub>2</sub> batteries with a N-CNTs@Ti cathode and a CNT powder cathode, respectively [111]. (For interpretation of the references to color in this figure legend, the reader is referred to the web version of this article.)

Therefore, it is an appealing option to coat defect-rich CQD on a suitable conductive substrate to enhance its electrocatalytic activity [114–116]. Dai et al. [117] prepared the first CQD/hG nanosheet composite catalyst by  $\pi$ - $\pi$  stacking. CQD/hG-0.3 (weight ratio of CQDs:hG = 0.3:1 wt%) material showed that CQDs with size of 5–10 nm were uniformly dispersed on plane of the porous graphene sheet (Fig. 6a–b). Compared with pure hG, the defects of CQD/hG-0.3 catalyst increased (Fig. 6c), and the significant increase in C–O peak composition indicated that the oxygen-enriched CQD was successfully anchored on the hG nanosheet (Fig. 6d–e). The effective formation and decomposition of Li<sub>2</sub>CO<sub>3</sub> during the charge/discharge process is attributed to the synergy between the CQD and hG components (Fig. 6f–h). When the current density is 0.5 A g<sup>-1</sup>, the discharge capacity is 12300 mAh g<sup>-1</sup> (Fig. 6i). At a current density of 0.1 A g<sup>-1</sup>, the overpotential is as low as 1.02 V (Fig. 6j). At a current density of 1 A g<sup>-1</sup>, the cycle stability is as high as 235 cycles (Fig. 6k), and the cut-off capacity is 500 mAh g<sup>-1</sup>.

In this section, the effects of different carbon-based catalytic materials, such as commercial carbon materials, one-dimensional carbon tubes and two-dimensional graphene, on the Li-CO<sub>2</sub> electrochemical performance were summarized. Indeed, the design of various defects, such as

voids, edges and doped heteroatoms to enhance the performance of the C materials were discussed. Accordingly, it can be concluded that although C materials have a low cost, their performance cannot meet the requirements of practical Li-CO<sub>2</sub> batteries, so that more efficient and practical catalytic materials need to be studied to address all the issues.

### 3.2. Noble metal-based catalyst

Precious metal catalysts are highly valued for their excellent activity, selectivity, stability, and are widely used in environmental protection and new energy fields [118,119]. Precious metal catalysts have many applications in Li-air, Li-O<sub>2</sub> and Li-CO<sub>2</sub> batteries [120–125]. Ru is a precious metal catalyst with wide application prospects. It has an excellent catalytic activity and is a promising catalyst that can promote the reversible reaction of CO<sub>2</sub>. Zhou et al. first used Ru nanoparticles as Li-CO<sub>2</sub> battery catalysts [90]. They used a solvothermal method to deposit Ru nanoparticles (particle size estimated to be about 5–10 nm) on Super P. The Ru content in Ru@Super P was estimated to be 15 wt%, and the obtained material showed a better electrochemical performance. It can deliver a discharge capacity of 8229 mAh g<sup>-1</sup> with a

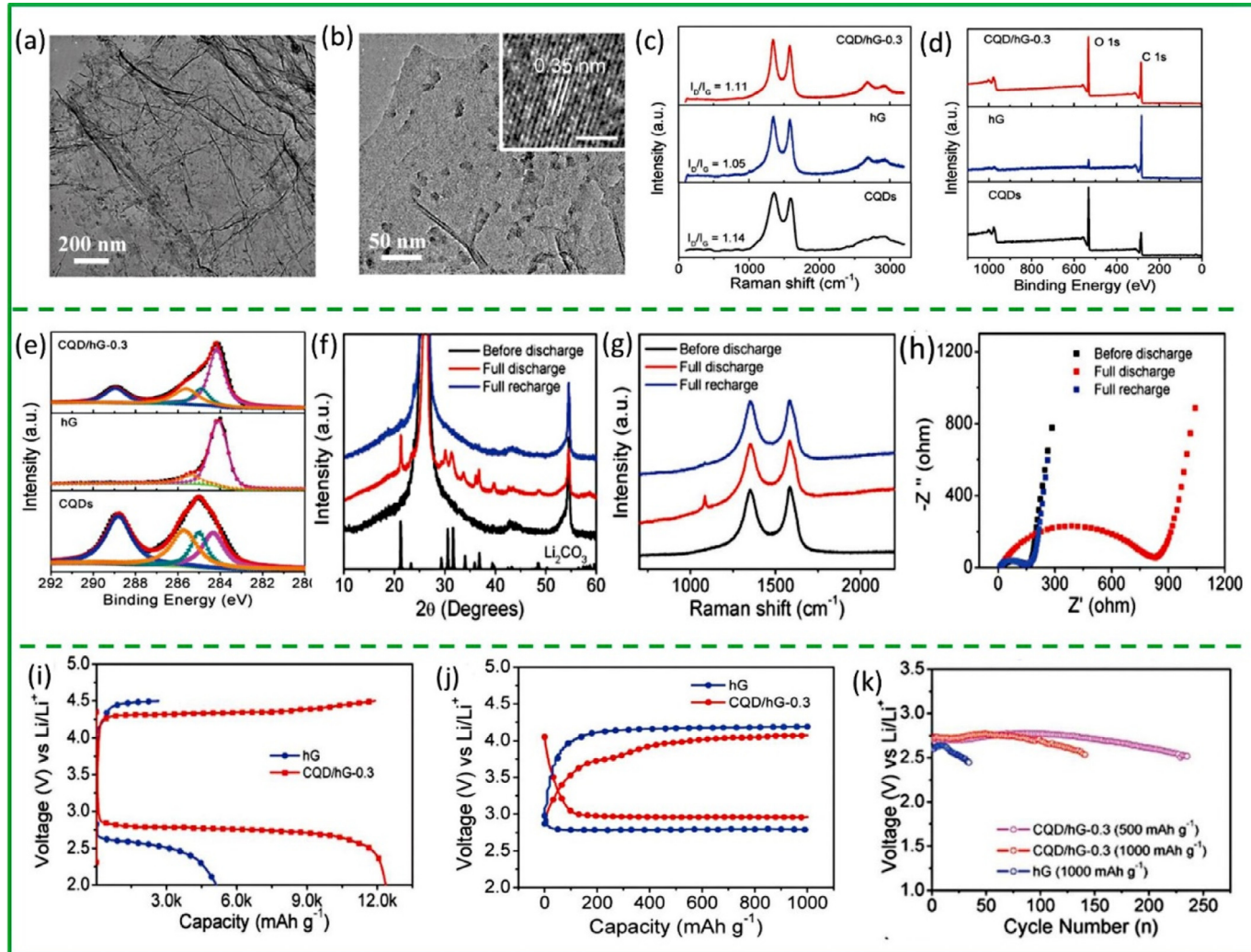


**Fig. 6.** (a) TEM image of CQD/hG-0.3 catalyst. (b) HRTEM of CQDs (inset, 2 nm scale). (c) Raman spectrum, (d) XPS spectrum, and (e) High resolution XPS spectra of C 1D for CQDs, hG and CQD/hG-0.3 catalysts. (f) XRD pattern, (g) Raman spectrum, (h) EIS spectrum, (i) Complete discharge curve, and (j) The first discharge-charge curve of Li-CO<sub>2</sub> battery based on hG and CQD/hG-0.3 catalyst. (k) Long cycle stability [117].

coulombic efficiency of 86.2% in the first cycle of the full discharge-charge test. Indeed, it can cycle over 70 times with a cut-off capacity of 1000 mAh g<sup>-1</sup> at current densities of 100, 200 and 300 mA g<sup>-1</sup>. In situ SERS and GC-MS results show that Ru nanoparticles can significantly promote the reaction between Li<sub>2</sub>CO<sub>3</sub> and C during the charging, and reduce the charging voltage from 4.5 V to 3.8 V. Chen et al. developed monodisperse Ru nanoparticles (with an average particle size of 2 nm) functionalized graphene nanosheets as an effective cathode catalyst [79]. It could effectively promote the decomposition of Li<sub>2</sub>CO<sub>3</sub> at a charge potential of 4.02V, thereby achieving relatively high coulombic efficiency and good cycle stability.

Zhou et al. designed a highly co-dispersed ruthenium-copper nanoparticle on graphene (Ru-Cu-G) as an effective air cathode for Li-CO<sub>2</sub> batteries [126]. The two metals are highly monodisperse on graphene (Fig. 7a-c). Selected area electron diffraction (SAED) mode shows typical polycrystalline diffraction rings of Ru and Cu (Fig. 7d). Compared with Ru-G and Cu-G, the structural changes of Ru-Cu-G before and after calcination are shown in Fig. 7e. The synergy between Ru and Cu makes the structure stable for a long time and results in a better electrochemical performance. With a rate of 200 mA g<sup>-1</sup> and a fixed capacity of 1000 mAh g<sup>-1</sup>, Ru-Cu-G can achieve a very stable cycling in 100 cycles and has a low overpotential of less than 0.88 V. Even at a high current density of 400 mA g<sup>-1</sup>, the discharge capacity of Ru-Cu-G

can still provide 13,590 mAh g<sup>-1</sup>, with a coulombic efficiency of 96.0% and cycle efficiency of 61.2% under the cutoff voltage of 4 V. More importantly, after long-term cycling, Ru-Cu-G still maintains a 3D porous structure without accumulated discharge products, which is essential for the stable operation of Li-CO<sub>2</sub> batteries.

Wang et al. used a simple replacement reaction method to synthesize three-dimensional nickel foam loaded Ru (Ru/Ni) catalyst as a binder free cathode for Li-CO<sub>2</sub> batteries [127]. The highly dispersed Ru nanosheets in the Ru/Ni cathode effectively promote decomposition of the discharge product Li<sub>2</sub>CO<sub>3</sub>, thereby reducing the charge overpotential. It exhibits a discharge capacity of 9502 mAh g<sup>-1</sup> and a coulombic efficiency of 95.4% at a current density of 100 mA g<sup>-1</sup>, which is much better than those of the KB/Ni electrode (5840 mAh g<sup>-1</sup> with an inferior coulombic efficiency of 13.8%). Meanwhile, the Ru/Ni catalytic cathode also shows a good rate performance (3177 mAh g<sup>-1</sup> at a current density of 500 mA g<sup>-1</sup>). Moreover, when operated at the limited capacity of 1000 mAh g<sup>-1</sup>, the battery can be stably discharged-charged for over 100 cycles while the corresponding charge potential is as low as 4.1 V.

Hu et al. reported ultra-fine Ru nanoparticles on activated carbon nanofibers (ACNFs) as an effective cathode for Li-CO<sub>2</sub> battery [128]. ACNF's porous and defect-rich structure caused high dispersion of Ru nanoparticles with small and narrow size distribution (4.1 ± 0.9 nm) (Fig. 7f). SEM and TEM images show that Ru nanoparticles are evenly

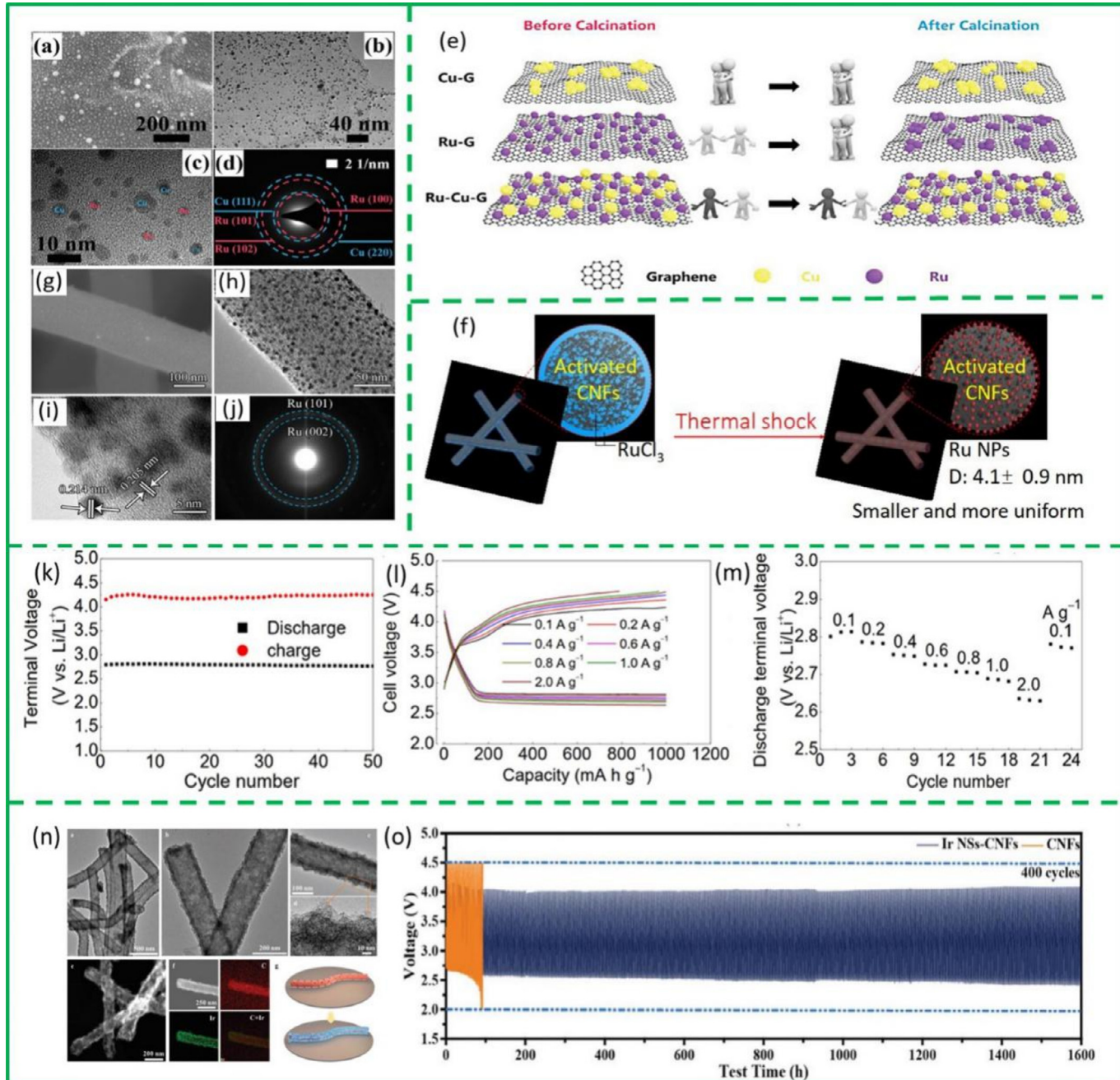


**Fig. 7.** Ru-Cu-G: (a) SEM, (b) TEM, (c) HRTEM images and (d) SAED mode. (e) Schematic representation of changes in Cu-G, Ru-G, and Ru-Cu-G before and after calcination [126]. (f) Schematic diagram of Ru nanoparticle formation on ACNF by transient thermal shock synthesis. (g) SEM images, (h) TEM images, (i) HRTEM image and (j) SAED mode of Ru/ACNFs, which indicates the polycrystalline structure of ruthenium nanoparticles. (k) Discharge and charge terminal voltage during cycling, (l) Charge/discharge curves at different current densities, (m) the final discharge voltage at different current densities [128]. (n) TEM image, high-resolution TEM image, high-angle annular dark-field scanning TEM image, element mapping and schematic illustration of the Ru/ACNF cathode. (o) Cycle performance of Li-CO<sub>2</sub> battery with Ir NSs-CNFs and CNFs as cathodes at a current density of 500 mA g<sup>-1</sup> and a limited capacity of 1000 mAh g<sup>-1</sup> [94].

distributed on ACNFs (Fig. 7g-h). High-resolution TEM and SAED images show that hexagonal structured Ru has high crystallinity (Fig. 7i-j). Ru has a higher loading on/in the ACNF substrate (content 18.1 wt%). The batteries show good electrochemical performance, with an initial discharge capacity of 11495 mAh g<sup>-1</sup>, a reversible charge capacity of 10715 mAh g<sup>-1</sup>, and an initial energy efficiency of 93.2%. After 50 cycles at 0.1 A g<sup>-1</sup>, the electrode showed a low overpotential of 1.43 V (Fig. 7k). Even at current densities of 0.8 and 1.0 A g<sup>-1</sup>, low overpotentials of 1.79 and 1.81 V can be achieved (Fig. 7l). Meanwhile, Li-CO<sub>2</sub> batteries with Ru/ACNF cathodes are highly reversible. After cycling

under high current density, when the current density decreased to 0.1 A g<sup>-1</sup>, the discharge terminal voltage returned to 2.77 V (Fig. 7m).

The above-mentioned study shows that Ru nanoparticles can promote the reaction between Li<sub>2</sub>CO<sub>3</sub> and C, and effectively reduce the overpotential between CO<sub>2</sub>RR and CO<sub>2</sub>ER. Liu et al. demonstrated that RuO<sub>2</sub> has also an excellent catalytic ability for Li-CO<sub>2</sub> batteries [129]. They used RuO<sub>2</sub> decorated CNTs as cathode materials. CNT@RuO<sub>2</sub> composite materials can not only deliver a high specific capacity, but also provide a lower charging voltage (3.9 V). With the CNT@RuO<sub>2</sub> cathode, the coulombic efficiency remained around 100% until the 15<sup>th</sup> cycle.

Additionally, the morphology of the discharge product was needle-like, and  $\text{Li}_2\text{CO}_3$  did not seem to grow along the surface of the CNT@ $\text{RuO}_2$  composite. The battery can maintain 55 cycles, and the charging voltage of the initial 30 cycles can be fully controlled below 4.0 V. Nonetheless, the mechanism of the discharge reaction in the CNT@ $\text{RuO}_2$  cathode is not clear, and further in-situ characterization is needed for more investigations. Recently, Wang et al. designed  $\text{RuP}_2$  nanoparticles highly dispersed on N, P double doped C film ( $\text{RuP}_2\text{-NPCF}$ ) for Li- $\text{CO}_2$  battery [130]. The battery can provide a reversible discharge capacity of  $11951 \text{ mAh g}^{-1}$  and achieve a better cycle capability of more than 200 cycles with a low overpotential (<1.3 V) at a fixed capacity of  $1000 \text{ mAh g}^{-1}$ .

In addition to Ru-based catalysts, metal Ir-based catalysts have attracted widespread attention in Li- $\text{O}_2$  batteries and electrocatalysis [131]. Metal Ir-based materials have been shown to effectively promote oxygen reduction reactions (ORR) and oxygen release reactions (OER) [132–134]. A study on Li-air batteries has proven that Ir/ $\text{B}_4\text{C}$  materials can decompose  $\text{Li}_2\text{CO}_3$  at a voltage below 4.37 V and the efficiency can reach 100% [135]. Zhou et al. successfully fabricated Ir/CNFs as the air cathode of Li- $\text{CO}_2$  battery by electrostatic spinning [136]. For the first time, the precious metal Ir was applied for Li- $\text{CO}_2$  battery. Benefiting from the high catalytic activity of Ir nanoparticles and the unique porous network of Ir/CNFs, the Li- $\text{CO}_2$  battery showed a very high discharge capacity of  $21528 \text{ mAh g}^{-1}$  and a coulombic efficiency of 93.1% in the first full discharge test. The battery also had an excellent cycle stability and a stable discharge and charging platform. Ectopic characterization showed that Ir/CNFs affects the morphology of the discharge products by enhancing them to granular instead of polymer, which is beneficial for reducing the overpotential. The independent Ir/CNF film has a relatively high energy density ( $11.54 \text{ mAh cm}^{-1}$ ) and a comparatively long cycle life (over 1200 hours). Guo et al. manufactured a class of high-density wrinkled Ir nanosheets covering the surface of N-doped, highly porous carbon nanofibers (Ir NSS-CNFs) as an effective cathode for improving the performance of Li- $\text{CO}_2$  batteries [94]. The ultra-thin (<1 nm) and wrinkled Ir nanoplatelets uniformly and completely cover the surface of the porous CNF (Fig. 7n), which may effectively protect the C matrix from decay, because the free radicals generated during the charging/discharging process will corrode the C material and form different by-products. The two-dimensionally wrinkled and ultra-thin Ir nanosheets can expose more available active sites in electrochemical reactions. This unique structure is essential for boosting the capacity and stability of Li- $\text{CO}_2$  battery. The battery can be stably discharged at least 400 times, with a current density of  $500 \text{ mA g}^{-1}$  and a cut-off capacity of  $1000 \text{ mAh g}^{-1}$  (Fig. 7o). Meanwhile, the cathode can effectively reduce the charge overpotential by showing a charge termination voltage below 3.8 V at  $100 \text{ mA g}^{-1}$ . Evidently, metal Ir can improve the CO<sub>2</sub>RR and CO<sub>2</sub>ER of Li- $\text{CO}_2$  battery. However, participation of C in the reaction of  $\text{Li}_2\text{CO}_3$  needs further research.

Based on Ir's excellent catalytic activity, Xie et al. introduced  $\text{IrO}_2$  to Li- $\text{CO}_2$  batteries [73]. They prepared ultrafine  $\text{IrO}_2$  modified thin-layer  $\delta\text{-MnO}_2$  catalyst ( $\text{IrO}_2/\text{MnO}_2$ ), which was directly grown on carbon cloth (CC). The catalytic activity of  $\text{IrO}_2/\text{MnO}_2$  can reversibly deposit/remove a thin layer of amorphous  $\text{Li}_2\text{CO}_3$  on the surface of  $\text{IrO}_2/\text{MnO}_2$  nanoflakes. As a result, the Li- $\text{CO}_2$  battery shows a good electrochemical performance by providing a high capacity of  $6604 \text{ mAh g}^{-1}$  at  $100 \text{ mA g}^{-1}$ . Under the capacity limit of  $1000 \text{ mAh g}^{-1}$ , it can maintain a stable cycle of more than 300 cycles at  $400 \text{ mA g}^{-1}$ . After 200 cycles, the high capacity of  $1070 \text{ mAh g}^{-1}$  was still maintained while the current density was  $800 \text{ mA g}^{-1}$ . Nonetheless, the presence of any interactions between  $\text{IrO}_2/\text{MnO}_2$  and the formation mechanism of amorphous discharge products is still unclear.

According to this section, Ru and Ir as two precious metal catalysts can effectively reduce the charge overpotential, preventing the electrolyte from decomposing within the working potential range, and improving the cycle performance and rate performance of Li- $\text{CO}_2$  battery. However, because the precious metals are rare and costly, their indus-

trial and large-scale production is difficult to achieve, which limits their practical application in Li- $\text{CO}_2$  batteries to a certain extent.

### 3.3. Transition metal compound-based catalysts

Although precious metal catalysts have excellent catalytic activity and can effectively promote  $\text{CO}_2$  reduction and precipitation reactions, their high cost as energy materials contradicts their practical application. Therefore, the development of cheap and abundant non-precious metal catalysts is expected to be an effective strategy to solve these problems [137–142]. Due to the multivalent nature of transition metal and its good activity in the field of electrocatalysis, many researchers have investigated its application in Li- $\text{CO}_2$  batteries [143–147]. Transition metal oxides (TMOs) with moderately high-valent metal atoms are considered as an economical and effective option due to their low cost and rich content [148]. According to previous studies, NiO can be used to decompose carbonate/carboxylate species in Li- $\text{O}_2$  batteries to reduce the accumulation of byproducts, while considered to be effective in catalytic decomposition of  $\text{Li}_2\text{CO}_3$  as well [149,150]. Zhou et al. introduced NiO to Li- $\text{CO}_2$  batteries for the first time [151]. The NiO-CNT composite is composed of plentiful interconnected CNTs and hexagonal polycrystalline NiO nanosheets adhered thereto (Fig. 8a). Li- $\text{CO}_2$  batteries with this material as cathode show an excellent electrochemical performance due to its special structure and high specific surface area. NiO-CNT composites have enhanced  $\text{Li}_2\text{CO}_3$  decomposition activity (Fig. 8b). It delivers a discharge capacity of  $9000 \text{ mAh g}^{-1}$  with a high coulombic efficiency of 97.8% in the first cycle at a current density of  $100 \text{ mA g}^{-1}$ . The NiO-CNT cathode shows a stable 2.7 V discharge platform and a 4.1 V low-charge platform. In the 5<sup>th</sup> cycle, the battery shows a capacity of  $6437 \text{ mAh g}^{-1}$  with a coulombic efficiency of 91.7% (Fig. 8c), indicating that  $\text{Li}_2\text{CO}_3$  can be effectively decomposed (Fig. 8d). Moreover, Li et al. [152] proposed a simple strategy for preparing porous NiO nanofibers (NiO NFs) by combining electrospinning technology and heating method, and successfully used it as a cathode catalyst for Li- $\text{CO}_2$  batteries. Experimental results combined with DFT calculation show that the presence of porous NiO NFs increases the contact area between the discharge product and the electrode, thereby maximizing the use of catalytic active sites, promoting the decomposition of  $\text{Li}_2\text{CO}_3$ , and also promotes diffusion of electrons and reactants. Meanwhile, XRD analysis shows that the NiO catalyst is stable during cycling. Therefore, non-noble metal NiO-based catalysts have far-reaching significance in improving the electrochemical performance of the battery.

In addition to nickel-based oxides, as the widely studied TMO series, Mn-based oxides with various valence states and structural tunability have attracted more and more attention due to their catalytic activities in ORR, OER and CO<sub>2</sub>RR, [153,154] as well as their huge potential as cathode catalysts for rechargeable Li- $\text{CO}_2$  batteries. Liu et al. prepared porous  $\text{Mn}_2\text{O}_3$  ( $\text{P-Mn}_2\text{O}_3$ ) as a low-cost cathode catalyst for Li- $\text{CO}_2$  battery by the sol-gel method [155]. The highly porous structure of  $\text{P-Mn}_2\text{O}_3$  gives it interconnected channels for mass transfer, good gas/liquid/solid reaction interfaces, and proper voids for containing discharge products. The prepared  $\text{P-Mn}_2\text{O}_3$  has a long-lasting high catalytic activity for CO<sub>2</sub> electrochemical redox in Li- $\text{CO}_2$  batteries with the duration of more than 2000 h at a current density of  $50 \text{ mA g}^{-1}$ , while the polarization intensity is only 1.4 V. SEM, XRD, FTIR, Raman spectroscopy, and XPS demonstrate the reversible formation and decomposition of  $\text{Li}_2\text{CO}_3/\text{C}$  species during battery cycling, rather than the separate decomposition of  $\text{Li}_2\text{CO}_3$  (Fig. 8e-f). In addition, Raman spectroscopy and XPS clarified that the C product obtained on the discharged  $\text{Mn}_2\text{O}_3$  cathode shows a highly graphitized characteristics, which is different from the results reported in other studies [156–158]. Peng et al. prepared a new type of Co-doped  $\alpha\text{-MnO}_2$  nanowires on CC through a simple hydrothermal reaction [158]. Li- $\text{CO}_2$  battery using optimized  $\text{Co}_{0.2}\text{Mn}_{0.8}\text{O}_2/\text{CC}$  cathode electrodes exhibited a high capacity ( $8160 \text{ mAh g}^{-1}$  at a current density of  $100 \text{ mA g}^{-1}$ ), low overpotential ( $\approx 0.73$

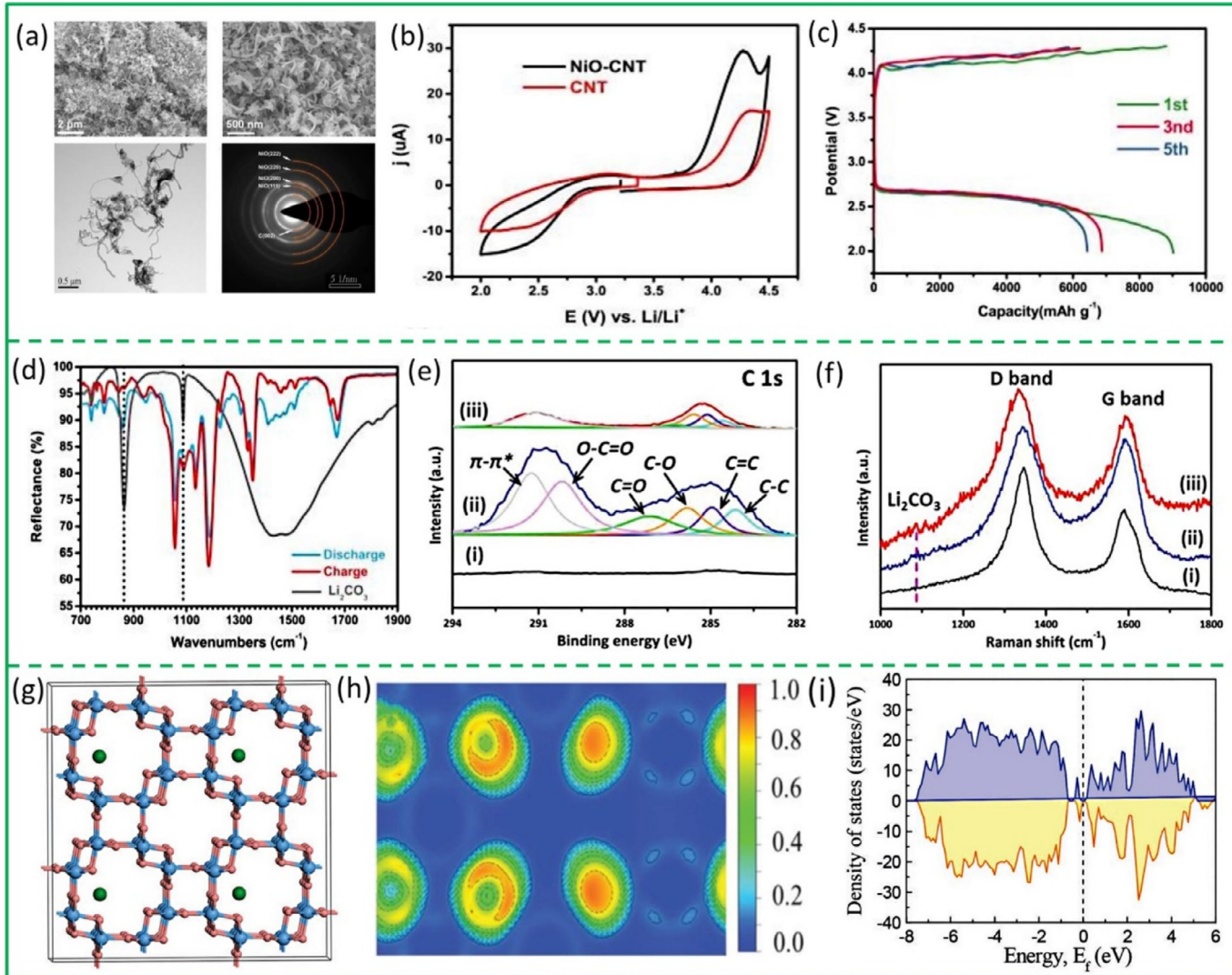


**Fig. 8.** (a) SEM image, TEM image and SAED pattern of NiO-CNT. (b) CV curve. (c) The discharge curve of NiO-CNT cathode in Li-CO<sub>2</sub> batteries at a current density of 50 mA g<sup>-1</sup>. (d) FTIR spectrum of a discharged and charged NiO-CNT cathode [151]. (e) C 1s XPS spectra of the KB-free P-Mn<sub>2</sub>O<sub>3</sub> electrode. (f) Raman spectra of the P-Mn<sub>2</sub>O<sub>3</sub>/KB electrode [155]. (g) Theoretical interpretation, (h) DOS and (i) ELF images of Co-doped  $\alpha$ -MnO<sub>2</sub> (interstitial III position) [158].

V) and long cycle life (over 500 cycles at a current density of 100 mA g<sup>-1</sup>). The effects of co-doped sites on the electrochemical performance of  $\alpha$ -MnO<sub>2</sub> were studied by first-principle calculations, including co-doped occupied sites (Fig. 8g), state density (DOS), and electron local function (ELF). Co-doping can significantly reduce Fermi energy. In particular, the co-gap site (Gap III) considerably shortened the band gap of  $\alpha$ -MnO<sub>2</sub> to form an impurity band (Fig. 8i), and then enhanced the conductivity of  $\alpha$ -MnO<sub>2</sub> with a narrow energy band gap. In Co-doped MnO<sub>2</sub>, the electron pairs of Mn significantly increased (Fig. 8h), which indicates that the valence bond characteristics of Mn-O become weaker, while the ionic characteristics of Mn-O become stronger, resulting in an increase in electrical conductivity. Based on in-situ experimental observations and DFT calculations, they confirmed that the superior electrochemical performance is primarily related to high conductivity, enhanced BET specific surface area, and unique co-interstitial doping, which may be beneficial for CO<sub>2</sub> diffusion and the reversibility of Li<sub>2</sub>CO<sub>3</sub> products.

Except for the above-mentioned two oxides, anatase-type TiO<sub>2</sub> has also been shown to have bifunctional catalytic activity. It can be used as both a CO<sub>2</sub> trapping agent [159] and an electrochemical reducing agent [160]. The anatase-type TiO<sub>2</sub> has high CO<sub>2</sub> binding energy and excellent CO<sub>2</sub> adsorption capacity [161]. Because of these advantages, Manthiram's group turned their attention to anatase TiO<sub>2</sub> as a cathode catalyst

for Li-CO<sub>2</sub> batteries [162]. They prepared anatase-type titanium dioxide nanoparticles (TiO<sub>2</sub>-NPs)/CNT/CNF composites by a simple hydrolysis method. Anatase TiO<sub>2</sub>-NPs are precious metal-free catalysts that can attach, reduce, and release CO<sub>2</sub> during cycling. The batteries achieve a vastly improved cycling stability, showing no decrease in the discharge voltage (2.8 V) and only a marginal increase in the charge voltage (4.3 V - 4.4 V) over 20 discharge/charge cycles. However, the battery with the bare CNT/CNF cathode fails within 10 cycles.

Transition metal carbides have also attracted widespread attention. They are intermetallic filling compounds formed by interstitial melting of C atoms into the transition metal lattice. The study found that transition metal carbides have catalytic effects in many fields, and their surface properties and catalytic activities are similar to those of noble metals such as Pt. They are called "quasi-platinum catalysts". Mo<sub>2</sub>C has been widely studied for its excellent catalytic properties. It is similar to metals in Group VIII and has attracted broad attention for methane conversion [163], water-gas shift reaction [164], hydrogen evolution reaction [165,166], and CO<sub>2</sub>RR [167]. Compared with Mo, high activity of Mo<sub>2</sub>C is derived from the electronic properties introduced by C, which affects the binding energy of Mo-C and the reactivity of the adsorbate. As a catalyst for Li-O<sub>2</sub> battery, Mo<sub>2</sub>C has high electrical efficiency and reversibility due to its partially oxidized surface [168]. In view of

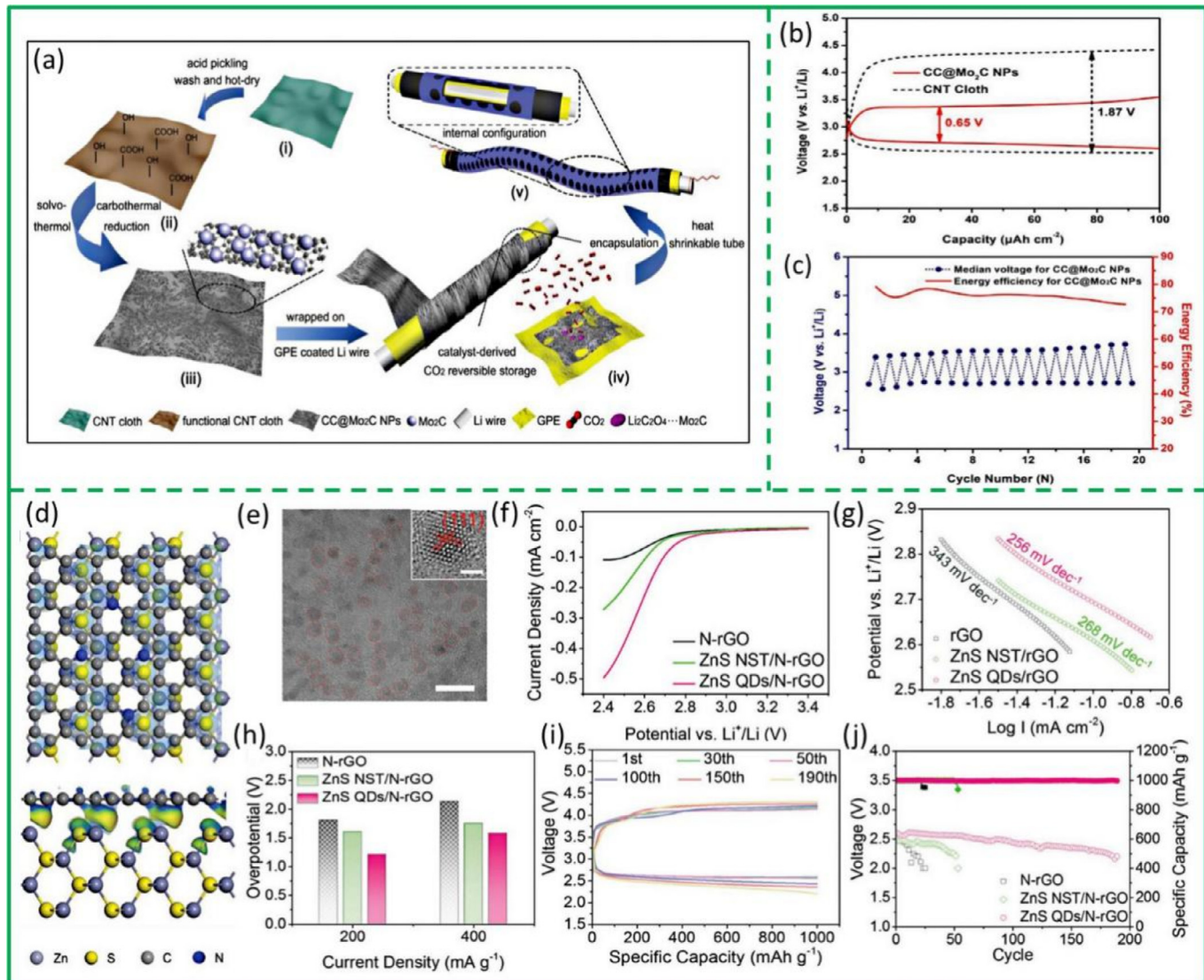


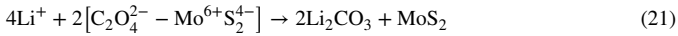
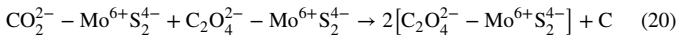
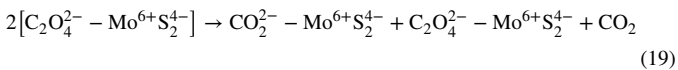
**Fig. 9.** (a) Preparation of flexible fibrous Li-CO<sub>2</sub> batteries using CC@Mo<sub>2</sub>C NPs independent membrane as cathode. (b) Comparison of CC@Mo<sub>2</sub>C NP and CNT cloth electrodes with constant current discharge/charge curves in CO<sub>2</sub> with an initial capacity of 100  $\mu\text{Ah cm}^{-2}$ . (c) Median voltage of discharge/charge platform for CC@Mo<sub>2</sub>C NPs electrodes [95]. (d) Charge distribution calculated by density functional theory at the interface of ZnS QDs and N-rGO. (e) HR-TEM image of ZnS QDs/N-rGO (scale bar = 10 nm; scale bar illustration = 2 nm). (f) CO<sub>2</sub>RR catalytic activity and (g) Tafel curves in 1.0 M LiTFSI/TEGDME with N-rGO, ZnS NST/N-rGO and ZnS QDs/N-rGO as catalysts. (h) Mean overpotential at 200 mA g<sup>-1</sup> and 400 mA g<sup>-1</sup>. (i) Discharge/charge voltage curve of ZnS QDs/N-rGO cathode. (j) Long-term cycling performance of Li-CO<sub>2</sub> batteries [173].

the Mo<sub>2</sub>C excellent catalytic performance, Chen et al. prepared Mo<sub>2</sub>C through a carbothermal reduction process and used it as a catalyst for Li-CO<sub>2</sub> batteries [88]. With its 3D network of uniformly dispersed Mo<sub>2</sub>C nanoparticles as the catalytic site and CNTs as the conductive matrix, this cathode material shows a high round-trip efficiency of 77% and a good cycling performance. Through characterizations of the pure CNT and prepared Mo<sub>2</sub>C/CNT, it is indicated that reducing CO<sub>2</sub> in the presence of Mo<sub>2</sub>C follows a different approach, which can avoid the formation of insulating Li<sub>2</sub>CO<sub>3</sub>, thereby reducing the potential platform and improving Li-CO<sub>2</sub> battery round-trip efficiency. Mo<sub>2</sub>C can stabilize the discharge product Li<sub>2</sub>C<sub>2</sub>O<sub>4</sub>, which has been explained in the mechanism section. Based on these inspirations, Wang et al. [95] demonstrated a quasi-solid flexible fibrous Li-CO<sub>2</sub> battery with low overpotential and high energy efficiency by using ultrafine Mo<sub>2</sub>C nanoparticles anchored on a CNT cloth free-standing hybrid film as a cathode (Fig. 9a). Due to the synergistic effect of the CNT substrate and Mo<sub>2</sub>C catalyst, it can achieve a low charge potential below 3.4 V (Fig. 9b), about 80% energy efficiency (Fig. 9c), and reversibly discharge and charge for 40 cycles.

Experimental results and theoretical simulations show that the intermediate discharge product Li<sub>2</sub>C<sub>2</sub>O<sub>4</sub>, which is stabilized by coordination electron transfer of Mo<sub>2</sub>C, is responsible for reducing the overpotential. Indeed, transition metal carbides with mid-valent metal atoms seem to be more cost-effective. It can stabilize CO<sub>2</sub>RR in the two-electron transfer stage and prevent the subsequent disproportionation process from transferring to four electrons, which significantly reduces the overpotential of the current Li-CO<sub>2</sub> battery system.

In addition to transition metal oxides and carbides, transition metal sulfides have also attracted a lot of attention. MoS<sub>2</sub> has been recognized as an effective catalyst for enhancing redox kinetics in various battery chemistry [169–171]. Salehi-Khojin et al. employed MoS<sub>2</sub> in Li-CO<sub>2</sub> batteries for the first time [93], and used a single MoS<sub>2</sub> nanosheet as a cathode catalyst. The battery shows reversible cycling at 500 mAh g<sup>-1</sup> for 500 cycles, as well as a high charge/discharge capacity of 60000 mAh g<sup>-1</sup> at the first cycle. However, the overpotential is relatively high (>4 V) during charging, and the proposed catalytic mechanism is mainly supported by computational research. Subsequently, Manthiram et al. pre-

pared MoS<sub>2</sub> nanosheet (MoS<sub>2</sub>-NS)/multi-walled CNT/single-walled CNT nanocomposites through a simple hydrothermal reaction [172]. The Li-CO<sub>2</sub> battery prepared using free-standing MoS<sub>2</sub>-NS@MWNT/SWNT composite membrane as a CO<sub>2</sub> gas diffusion cathode can achieve 50 discharge/charge cycles with low overpotential, in which the discharge voltage is greater than 2.75 V and the charge voltage is less than 3.75 V. Apart from improving cycle stability and efficiency, the MoS<sub>2</sub> catalyst also increased the discharge capacity by about 50%. A series of characterization techniques supported the efficiency of catalytic mechanism for the formation and decomposition of Li<sub>2</sub>CO<sub>3</sub> on the surface of MoS<sub>2</sub>-NS Eq. (18)–(21). Indeed, reversible formation and decomposition of Li<sub>2</sub>CO<sub>3</sub> and C were achieved.



Almost at the same time, Wei et al. designed and synthesized a ZnS quantum dot/nitrogen-doped reduced graphene oxide (ZnS QDs/N-rGO) heterostructure as a gas electrode for Li-CO<sub>2</sub> battery [173]. ZnS QDs were uniformly adhered to the surface of the edge-wrinkled N-rGO with high coverage (Fig. 9e), leading to a strong interfacial interaction. The charge density at the ZnS QDs/N-rGO interface shows that electrons migrate from N-rGO to ZnS QDs (Fig. 9d). As shown in Fig. 9f-g, it was further confirmed that due to the strong interfacial interaction, ZnS QDs/N-rGO shows the largest initial potential among the samples along with a superior electron transfer efficiency for CO<sub>2</sub>RR. Compared with ZnS NST/N-rGO cathodes and N-rGO cathodes, Li-CO<sub>2</sub> battery with ZnS QDs/N-rGO cathodes have a lower average overpotential, e.g., at a current density of 200 mA g<sup>-1</sup> the average overpotential is 1.21 V (Fig. 9h). ZnS QDs/N-rGO cathodes show a small polarization, high round-trip efficiency and good cycling performance in Li-CO<sub>2</sub> batteries. Even at a constant current density of 400 mA g<sup>-1</sup>, they can operate stably for more than 190 cycles, with a limited capacity of 1000 mA g<sup>-1</sup> (Fig. 9i-j). The interface interaction has a positive effect on promoting the catalytic activity of Li-CO<sub>2</sub> batteries and controlling discharge products, and provides a new perspective for the design of rechargeable Li-CO<sub>2</sub> battery catalysts.

#### 3.4. MOF-COF-MPcs derivative catalyst

Metal-organic framework (MOF) is a porous material with rich structural versatility and functional tunability, and has been extensively studied in terms of CO<sub>2</sub> capture, separation, and catalytic conversion into useful compounds [174–177]. If the CO<sub>2</sub> captured in the pores of the MOF can be used for power supply, the environmental problems of C emissions can be mitigated, which is a highly desirable strategy [178]. Recently, Wang's group has identified the potential of MOF as a porous catalyst in Li-CO<sub>2</sub> batteries for the first time [179], owing to its high CO<sub>2</sub> capture capacity and Li<sub>2</sub>CO<sub>3</sub> decomposition of monodisperse active metal sites. They used six different MOF materials (Mn<sub>2</sub> (dobdc), Co<sub>2</sub> (dobdc), Ni<sub>2</sub> (dobdc), Mn (bdc), Fe (bdc) and Cu (bdc)) to screen out a metal center system with the ability to charge the Li-CO<sub>2</sub> system. The study found that Mn<sub>2</sub> (dobdc) materials exhibit a lower charge potential, and it is presumed that Mn (II) centers may play a positive role in activating Li<sub>2</sub>CO<sub>3</sub> after charging. Mn<sub>2</sub> (dobdc) reaches a high discharge capacity of 18022 mAh g<sup>-1</sup>, and the charge potential is as low as 3.96 V at 50 mA g<sup>-1</sup>. Mn (HCOO)<sub>2</sub> has smaller pores and moderate isothermal heat of CO<sub>2</sub> adsorption relative to Mn<sub>2</sub> (dobdc). With a limited capacity of 1000 mAh g<sup>-1</sup>, it can maintain a low charge potential of 4.02 V

for more than 50 cycles even at a high current density of 200 mA g<sup>-1</sup>. It was found that Mn (II) centers can effectively catalyze the decomposition of discharge products. However, the insulation of MOF makes it challenging to further improve the rate performance and cycle life of the battery. They believe that the design of more powerful MOF-based CO<sub>2</sub> cathodes should consider the following three aspects: dispersed catalytic materials, fast electron transport and strong interconnection networks. The first two points indicate the activity of cathode in decomposition of Li<sub>2</sub>CO<sub>3</sub>, thereby determining the voltage hysteresis of the batteries and their influence will be more prominent at high current densities. The last point ensures the stability of the cathode when subjected to repeated deposition and decomposition of discharge products. Following the above principle, the research group prepared ultrafine MnO nanoparticles dispersed in interconnected N-doped 3D carbon framework/graphene composite (MnO@NC-G) (Fig. 10a) as cathode material for Li-CO<sub>2</sub> battery [91]. The octahedral MOF-derived MnO nanoparticles (in the range of 5 to 10 nm) were wrapped by ultra-thin graphene sheets (Fig. 10b-c). Owing to this rugged 3D structure, fast electronic transmission and mass diffusion were achieved. The MnO@NC-G cathode can achieve a low ΔV of 0.88 V at 50 mA g<sup>-1</sup> (Fig. 10d), a high rate capability of up to 1 A g<sup>-1</sup>, and a long cycle of more than 200 cycles under the action of 1000 mAh g<sup>-1</sup>. It can also provide a maximum discharge capacity of 25021 mAh g<sup>-1</sup> in the range of 2.0–4.5 V at 50 mA g<sup>-1</sup> (Fig. 10e), and 10 reversible cycles at 200 mA g<sup>-1</sup> with capacity limit of 5000 mAh g<sup>-1</sup>. After 200 cycles, the reassembled battery can be recycled for 176 cycles (Fig. 10f). The experimental results show that the cycle life of the battery can be further extended by the improvement of other components, especially the protection of Li-metal anodes.

Covalent organic framework (COF) is a new type of porous crystalline material [180–182]. The material's strong covalent bonds and easy-to-code features give it high stability, making it potentially useful as a light-emitting, catalytic, and energy storage material [183–185]. The ordered porosity in COF provides a tailored one-dimensional channel for gas storage and separation [186]. Studies have shown that COF has a catalytic effect on CO<sub>2</sub>. Meng et al. used COF as a porous cathode catalyst in Li-CO<sub>2</sub> batteries for the first time [187]. They successfully designed and manufactured graphene@COF, which is a graphene with a thin and uniform imine COF loading that can enrich and limit CO<sub>2</sub>. The discharge voltage increases by a higher local CO<sub>2</sub> concentration, which is predicted by the Nernst equation and achieved by CO<sub>2</sub> nano-enrichment. In addition, the uniform Li-ion deposition guided by graphene@COF nano-constrained CO<sub>2</sub> can produce smaller Li<sub>2</sub>CO<sub>3</sub> particles, which leads to the easy decomposition of Li<sub>2</sub>CO<sub>3</sub> and reduces the charging voltage. The graphene@COF cathode with a C content of 47.5% delivered a discharge capacity of 27833 mAh g<sup>-1</sup> at 75 mA g<sup>-1</sup>. Indeed, a low charge potential of 3.5 V was maintained for 56 cycles under 0.5 A g<sup>-1</sup>. Meanwhile, Loh et al. used a hydrazine/hydrazide-containing COF to develop effective ion/gas diffusion channels for cathode materials in Li-CO<sub>2</sub> batteries [188]. The powerful one-dimensional channels in COF can act as CO<sub>2</sub> and Li-ion diffusion paths, and improve the kinetics of electrochemical reactions. The COF-based cathode exhibits a capacity of 27348 mAh g<sup>-1</sup> at a current density of 200 mA g<sup>-1</sup>. It has low cut-off overpotential of 1.24 V in the ultimate capacity of 1000 mAh g<sup>-1</sup>. The reduced overpotential indicates that the COF diffusion channel and Ru catalyst work together to reduce polarization. The rate performance can be significantly enhanced by using COF on the cathode, which shows a slow decay of the discharge voltage at a current density of 0.1 to 4 A g<sup>-1</sup>. COF-based batteries can run for 200 cycles when discharged/charged at a high current density of 1 A g<sup>-1</sup> while the discharge/charge voltage does not drop significantly. The use of COF as a cathode catalyst in Li-CO<sub>2</sub> battery makes it a potential candidate for energy storage equipment with high capacity and high rate performance.

Metal phthalocyanine (MPC) has been widely studied due to its unique metal center and promotion of CO<sub>2</sub> reduction reactions [189]. Based on density functional theory calculation, Illas's group [70] sys-

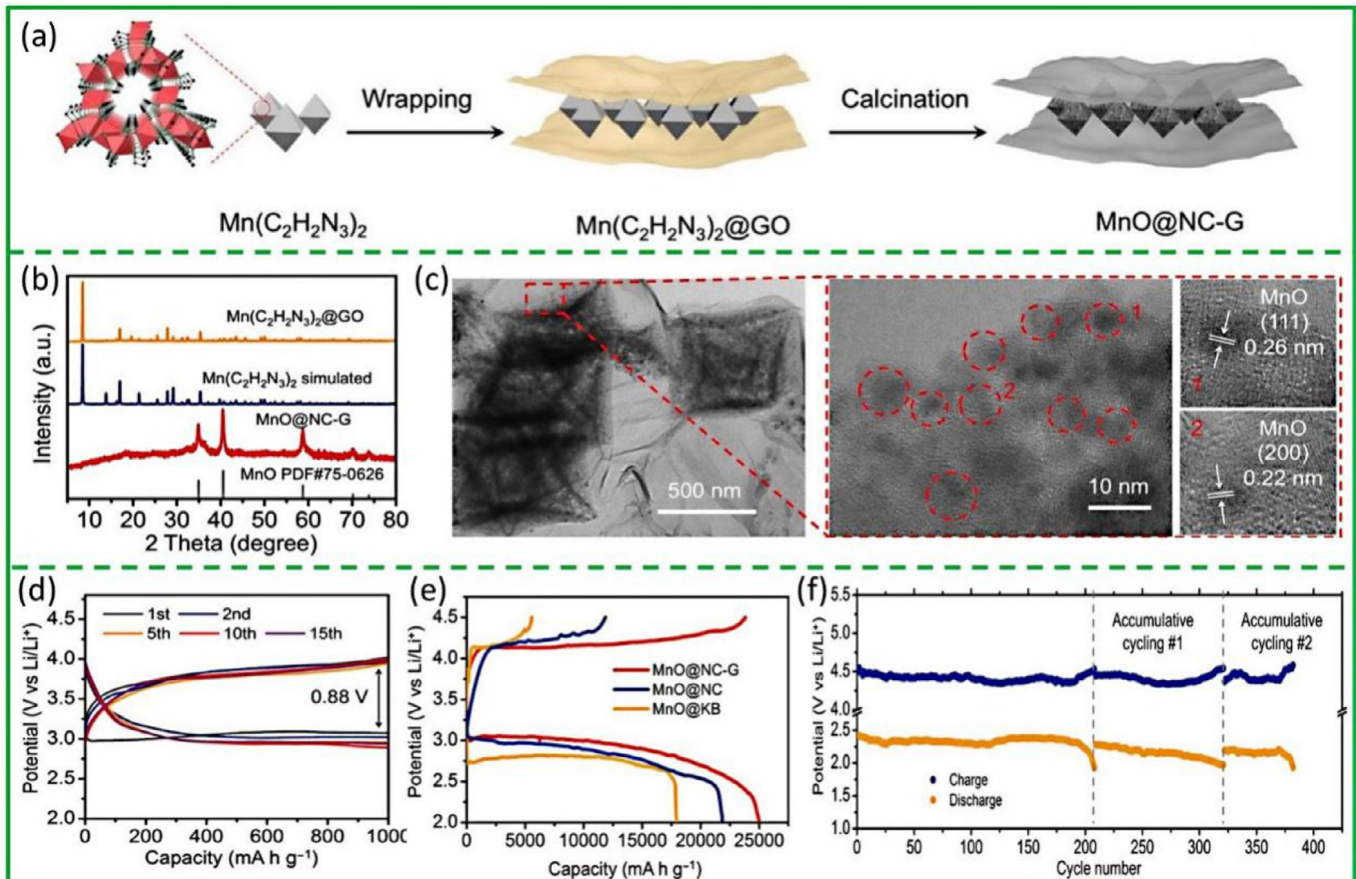


**Fig. 10.** (a) Synthesis of  $\text{MnO}@\text{NC-G}$ . (b) PXRD diagram of  $\text{MnO}@\text{NC-G}$ . (c) TEM and HRTEM images of  $\text{MnO}@\text{NC-G}$ . (d) Charge and discharge cycle performance of  $\text{MnO}@\text{NC-rGO}$  electrode at  $50 \text{ mA g}^{-1}$ . (e) Discharge curve at  $50 \text{ mA g}^{-1}$  and a voltage window of  $2.0\text{--}4.5 \text{ V}$ . (f) Using a fresh battery with fresh anode and electrolyte cycles to collect the cumulative number of cycles [91].

tematically added Li atoms and  $\text{CO}_2$  molecules to cobalt phthalocyanine (CoPc) nanosheets, realizing the feasibility of using the nanosheets as a molecular catalyst for cathodes in  $\text{Li-CO}_2$  batteries. Due to the high electron affinity of CoPc nanoplatelets, and the appropriate thermodynamics and kinetics of electron transfer from CoPc nanoplatelets to  $\text{CO}_2$  molecules during the formation of  $\text{Li}_2\text{C}_2\text{O}_4$  products, they demonstrated the potential of CoPc nanoplatelets as cathode catalysts in  $\text{Li-CO}_2$  batteries. Subsequently, Li et al. [190] reported the use of a convenient microwave heating method to synthesize conjugated cobalt polyphthalocyanine (CoPPc) polymers for  $\text{Li-CO}_2$  cathode materials. CoPPc has inherent elasticity and improved chemical, physical and mechanical stability due to the crosslinking network. CoPPc has a high catalytic activity for the formation and decomposition of reversible  $\text{Li}_2\text{CO}_3$ , so that the related high-performance  $\text{Li-CO}_2$  batteries possess a large capacity, minimal charge-discharge polarization, and impressive cycling performance.

According to the above studies, catalysts play an important role in determining the morphological structure and electrochemical reaction pathways of discharge products, and greatly affect the electrochemical performance of  $\text{Li-CO}_2$  batteries. However, as a more advanced electrochemical system, the exploration of catalysts in  $\text{Li-CO}_2$  batteries is still in its infancy. Therefore, finding a more effective catalyst is crucial for obtaining  $\text{Li-CO}_2$  batteries with superb reversible capacity, high energy efficiency and long cycle life.

#### 4. Electrolyte of $\text{Li-CO}_2$ batteries

Electrolyte, as an important part of  $\text{Li-CO}_2$  batteries, has a crucial impact on performance of the entire battery, including battery's cy-

cle stability, operating temperature range, and durability. Therefore, it is important to design an electrolyte with high ion conductivity, high number of ion migration, high stability and excellent mechanical properties. In the past few years, researchers have conducted a series of studies on various electrolytes. At present, there are two common electrolytes for  $\text{Li-CO}_2$  batteries. One is tetraethylene glycol dimethyl ether (TEGDME), containing lithium trifluoromethanesulfonate ( $\text{LiCF}_3\text{SO}_3$ ), and the other is lithium bis (trifluoromethanesulfonyl) imide ( $\text{LiTFSI}$ ) salt [191]. There are also several reports about organic electrolytes, such as dimethyl sulfoxide (DMSO) or trimethyl phosphate (TMP). Although these liquid electrolytes are able to promote  $\text{CO}_2$  degradation, they still cannot meet the requirements of high-efficiency and practical  $\text{Li-CO}_2$  batteries. The specific reasons are as follows: (1) these traditional liquid electrolytes may react with electrode materials during the cycle, resulting in capacity degradation; (2) the electrolyte may self-decompose under high charge potential; (3) lithium branches crystal growth is also affected, which may cause short circuits due to the uneven deposition of metallic lithium [192,193]. Therefore, it is necessary to continue to improve the electrolyte in order to obtain good electrochemical performance. In this section, electrolyte additives and solid/quasi-solid electrolytes will be discussed to promote a better and more effective  $\text{Li-CO}_2$  electrolyte design.

##### 4.1. Electrolyte additives

Previously, it has been proven that the addition of redox mediators to the electrolyte of  $\text{Li-O}_2$  batteries can reduce the overpotential to a certain extent [194–197]. Accordingly, Zhou et al. introduced a halide redox mediator ( $\text{LiBr}$ ) into the electrolyte of rechargeable  $\text{Li-CO}_2$  bat-

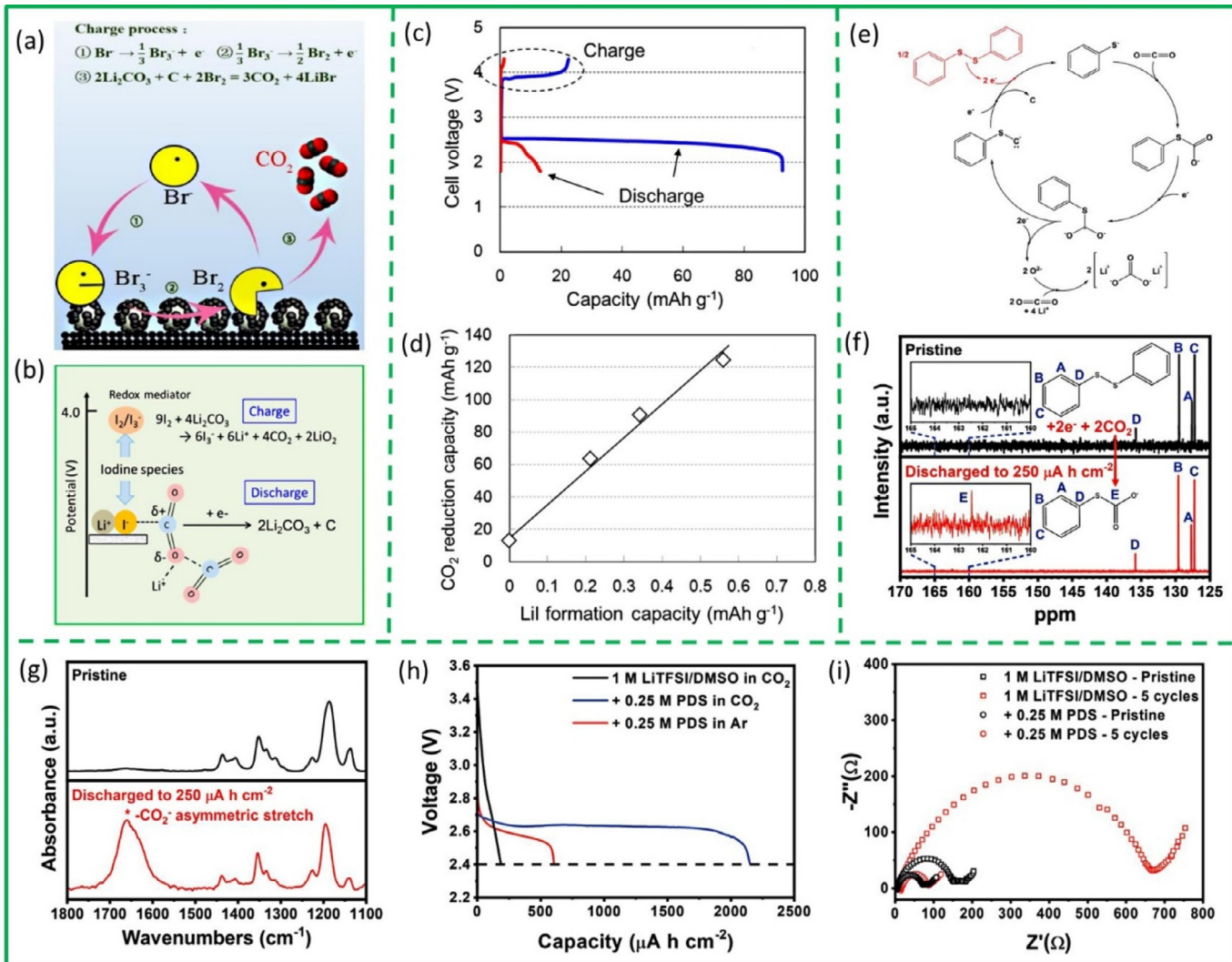


**Fig. 11.** (a) Proposed mechanism for the charging process using LiBr as a redox mediator [198]. (b) Charge-discharge mechanism of redox mediator of iodine species. (c) The first charge and discharge capacity using a CP cathode and 1MP L⁻¹ LiTFSI electrolyte in TMP (blue) and no I (red). (d) Relationship between CO<sub>2</sub> reducing ability and LiI forming ability during discharge [199]. (e) Mechanism of S-phenyl carbonothioate (SPC⁻)-mediated CO<sub>2</sub> reduction. (f) <sup>13</sup>C NMR and (g) FTIR-ATR Signal of 1 m LiTFSI+0.25 m PDS/DMSO electrolyte before and after partial discharge. (h) Comparison of discharge capacity. (i) Comparison of electrochemical impedance of Li-CO<sub>2</sub> batteries with and without 0.25 m PDS [204]. (For interpretation of the references to color in this figure legend, the reader is referred to the web version of this article.)

terry [198]. LiBr participates in the redox reaction during charge and discharge Fig. 11a). Moreover, the electrochemically produced Br<sub>2</sub> promotes the chemical decomposition of Li<sub>2</sub>CO<sub>3</sub> during the charging process. The reaction processes involved are shown in Eqs. (22)–(24).



At a current density of 50 mA g<sup>-1</sup>, the discharge capacity of the battery with LiBr is as high as 11500 mAh g<sup>-1</sup> with a coulombic efficiency of 81%. However, the discharge capacity of the battery without LiBr is about 2800 mAh g<sup>-1</sup>, and it is almost irreversible. At a current density of 100 mA g<sup>-1</sup> and a cut-off capacity of 500 mAh g<sup>-1</sup>, the battery can run stably for 38 cycles. At a current density of 200 mA g<sup>-1</sup>, a low charging voltage of around 4.0 V was observed, and the battery could operate for 16 cycles. It was proved that LiBr is favorable for the formation of the desired discharge product. Subsequently, Shiga et al.

added another halogen (iodine) as an additive to Li-CO<sub>2</sub> battery [199]. Compared with a common electrolyte, small amount of iodine additive can help to improve the discharge capacity (Fig. 11b). Lithium iodide (LiI) was first formed on the C cathode during discharge, and it was found that the reduction ability of CO<sub>2</sub> increases with the increase of LiI formation (Fig. 11c). They also investigated the catalytic activity of organic electrolyte systems for subsequent CO<sub>2</sub> conversion. Li<sub>2</sub>CO<sub>3</sub> accumulated on the cathode during the discharge process produces a passivation layer, which leads to a high charge overpotential (ca. 4.5 V vs Li<sup>+</sup>/Li). Compared with Li<sup>+</sup>/Li, iodine with a redox potential lower than 3.5 V cannot decompose Li<sub>2</sub>CO<sub>3</sub> because the decomposition potential of Li<sub>2</sub>CO<sub>3</sub> is 3.82 V. Nonetheless, the redox potential of iodine in trimethyl phosphate (TMP) electrolyte is greater than 3.8 V; thus, Li<sub>2</sub>CO<sub>3</sub> can be chemically decomposed by iodine in TMP. It was confirmed that the iodine mediator (3I<sub>2</sub>/2I<sup>3-</sup>) in the Li salt-TMP electrolyte can enhance the decomposition of Li<sub>2</sub>CO<sub>3</sub> at low charge voltages (Fig. 11d). The iodine species with a high redox potential play the role of redox medium, providing a useful means for its practical application in high energy density batteries.

In addition to inorganic materials (halogen salts) additives, organic compounds are also causing widespread concerns. Quinones represent a class of organic compounds with a variety of physicochemical properties, known for their high binding affinity for CO<sub>2</sub> in their reduced form, which have been used for concentration and selective separation of CO<sub>2</sub> [200]. Among these properties, it is found that their redox potential depends on their molecular structure and chemical environment [201]. Grimaud et al. studied three types of quinones with the aim of mediating CO<sub>2</sub> reduction, which was expected to result in lower overpotentials than direct electron transfer [202]. They found that when 2,5-ditert-butyl-1,4-benzoquinone (DBBQ) was added to the electrolyte, DBBQ divalent anions strongly interacted with CO<sub>2</sub>, which was due to its higher oxidation potential. The discharge voltage was determined by the reduction potential of DBBQ. However, battery performance and NMR analysis together indicated that side reactions involving quinone itself and other battery components have occurred. Thus, the limitations of using quinone to mediate the formation of Li<sub>2</sub>CO<sub>3</sub> in aprotic solvents have been proved, and it is further shown that the stability of the organic electrolyte solvents and their additives is crucial. Gallant et al. studied the use of a CO<sub>2</sub>-loaded amine solution as an electroactive electrolyte (amine-electrolyte combination) to promote the activity of the discharge reaction [203]. An alkylamine EEA-based CO<sub>2</sub> capture chemical was converted into a non-aqueous electrolyte, especially for DMSO, which is an electrolyte solvent found to have a negligible discharge capacity to reduce CO<sub>2</sub> on a C electrode. Subsequently, Manthiram et al. used phenyl disulfide (PDS) as an electrolyte additive in Li-CO<sub>2</sub> battery to achieve a solution-mediated CO<sub>2</sub> reduction pathway [204]. The discharge mechanism of Li-CO<sub>2</sub> battery doped with PDS is illustrated in Fig. 11e. After electrochemical reduction of PDS to generate thiophene anions, the adduct S-phenyl carbon sulfate (SPC<sup>-</sup>) is formed in the solution and used as a CO<sub>2</sub> trap. A mechanism for the capture and utilization of CO<sub>2</sub> mediated by SPC was proposed and supported by C<sup>13</sup> nuclear magnetic resonance spectroscopy and FTIR (Fig. 11f-g). Experimental results show that the solution-mediated pathway promotes the reversible formation and decomposition of Li<sub>2</sub>CO<sub>3</sub> and amorphous C during cycling. Li-CO<sub>2</sub> batteries utilizing PDS additives show a considerable improvement in capacity (Fig. 11h), energy efficiency and cycle life. Li-CO<sub>2</sub> batteries using 1 m LiTFSI+0.25 m PDS/DMSO as electrolyte show a lower charge transfer resistance compared to batteries using bare 1 m LiTFSI/DMSO (Fig. 11i). These researches pave the way for the development of cutting-edge electrolyte additives and long-life, high-efficiency Li-CO<sub>2</sub> batteries.

Although more research has been intended to demonstrate the enhanced Li-CO<sub>2</sub> battery performance provided by the electrolyte additive-mediated reaction pathway, there are fewer reports related to the effect of electrolyte salt concentration on electrochemical performance. Gallant et al. studied the effect of electrolyte composition on CO<sub>2</sub> discharge activity [205]. They found that TEGDME-based electrolytes with moderate concentrations of Li<sup>+</sup> salts (concentrations in the range of 0.7–2 M) are more favorable for CO<sub>2</sub> activation, especially compared to dimethylsulfoxide and propylene carbonate-based electrolytes. Through electrochemical, spectroscopic and computational methods, they determined that glymes have lower desolvation energies for Li<sup>+</sup> compared to other solvent candidates, whereas high salt concentrations increase the local density of Li<sup>+</sup> surrounding CO<sub>2</sub> and reduction intermediates. These attributes collectively increase Li<sup>+</sup> utilization, exceeding the threshold required to support CO<sub>2</sub> activation. The discharge voltage and reaction rate are also sensitive to the identity of alkali metal cations, further stimulating their key role in enabling or inhibiting the reactivity. These findings reveal the potential of developing alternative CO<sub>2</sub> reactive pathways through the future synthesis of novel electrolytes.

#### 4.2. Solid and quasi-solid electrolytes

Although the additives added to the liquid electrolyte are helpful for boosting the electrochemical performance of Li-CO<sub>2</sub> batteries,

these batteries still have some systematic key flaws in real-life application. For example, electrolyte evaporation, leakage, and flammability [206] severely limit the practical application of Li-CO<sub>2</sub> batteries with open systems and also the development of flexible batteries. The protection of Li anode is also controversial. Previous work reported that compared with pure O<sub>2</sub> atmosphere, Li metal anode can be protected in CO<sub>2</sub> atmosphere, relieve Li anode passivation and Li dendrite growth, which is the advantage of Li-CO<sub>2</sub> battery [207]. However, it is difficult to realize pure CO<sub>2</sub> atmosphere in practice (inevitable mixing of H<sub>2</sub>O, O<sub>2</sub>, etc.), coupled with the decomposition of the electrolyte, will still cause irreversible effects on Li-CO<sub>2</sub> batteries. In addition, the reactants of the CO<sub>2</sub> gas molecules have a high solubility in the liquid electrolyte, and it is easy to deposit thick, non-porous and polymer-like Li<sub>2</sub>CO<sub>3</sub>, which leads to a high overpotential. In order to overcome the shortcomings of liquid electrolytes, many researchers turned their attention to pure solid and quasi-solid electrolytes [208–210]. However, the pure solid electrolytes have a large impedance due to the contact between the solid interfaces, which is difficult to be applied in the open system of Li-CO<sub>2</sub> batteries. Therefore, gel-state electrolytes have received more attention.

Gel polymer electrolyte (GPE) is composed of a polymer matrix and a liquid electrolyte with a high ionic conductivity, close to liquid electrolytes [206,211]. Dense GPE can reduce the dissolution of CO<sub>2</sub> in water as well as the contact between Li anode and CO<sub>2</sub>. Wang et al. employed GPE in Li-CO<sub>2</sub> batteries for the first time [212]. GPE composed of a polymer matrix filled with a liquid electrolyte based on tetraethylene glycol dimethyl ether was used to manufacture a rechargeable Li-CO<sub>2</sub> battery with a CNT-based gas electrode. The Li<sub>2</sub>CO<sub>3</sub> discharge product formed in GPE-based Li-CO<sub>2</sub> battery showed a granular morphology with poor crystallinity, which is in contrast with the continuous polymer-like and crystalline discharge product in conventional Li-CO<sub>2</sub> batteries with a liquid electrolyte. As a result, GPE-based batteries demonstrate a significantly improved electrochemical performance. The achieved cycle life (60 cycles) and rate capability (maximum applied current density of 500 mA g<sup>-1</sup>) are much higher than the previously reported studies, which provides a new way to develop high-performance Li-CO<sub>2</sub> batteries. Subsequently, Guo et al. prepared a GPE containing 0.0025 M dinuclear cobalt phthalocyanine (Bi-CoPc-GPE) by a simple ultraviolet curing method as electrolyte [99]. Bi-CoPc-GPE has an excellent ionic conductivity (0.86 ms cm<sup>-1</sup>), effective protection for Li anodes and superb leak-proof performance. In addition, Bi-CoPc acts as a redox medium to promote the decomposition of discharge products at low charge potentials. Therefore, this polymer-based Li-CO<sub>2</sub> battery shows an ultra-high discharge capacity, almost 100% coulombic efficiency at the first cycle and low over-potential (1.4 V). Indeed, it can run stably for 120 cycles, while the Li-CO<sub>2</sub> battery with GPE only exhibits a specific capacity of 22570 mAh g<sup>-1</sup>, coulombic efficiency of <40% at the first cycle as well as a high over-potential (2.0 V), and it is not reproducible over 60 cycles. Yu et al. prepared a composite cathode composed of CNT and polymer electrolyte through in-situ polymerization process for solid-state Li-CO<sub>2</sub> batteries [213]. Because of the good dispersibility of CNT and polymer electrolytes, the Li-CO<sub>2</sub> battery has a high reversible capacity (11,000 mAh g<sup>-1</sup>) and excellent cycle stability at a low charge potential (4.5 V, 1000 mAh g<sup>-1</sup>, 100 cycles), which is better than those of liquid electrolyte-based batteries.

In view of the excellent performance of GPE, Wang et al. used N-CNTs@Ti-GPE-Li wire to assemble a quasi-solid flexible fibrous Li-CO<sub>2</sub> battery [111]. The manufacturing process is shown in Fig. 12a. The battery exhibits a high discharge capacity, improved cycle stability, and good rate performance. It is worth noting that the unique one-dimensional structure is quite easy to assemble (Fig. 12b). Additionally, this quasi-solid fibrous Li-CO<sub>2</sub> battery exhibits a high flexibility. As can be seen from Fig. 12c, when the bending angle range is 0–180°, the prefabricated fibrous Li-CO<sub>2</sub> battery will always light the red light-emitting diode (LED), and there is no evident brightness change during the deformation process. Interestingly, they also used another 10 cm

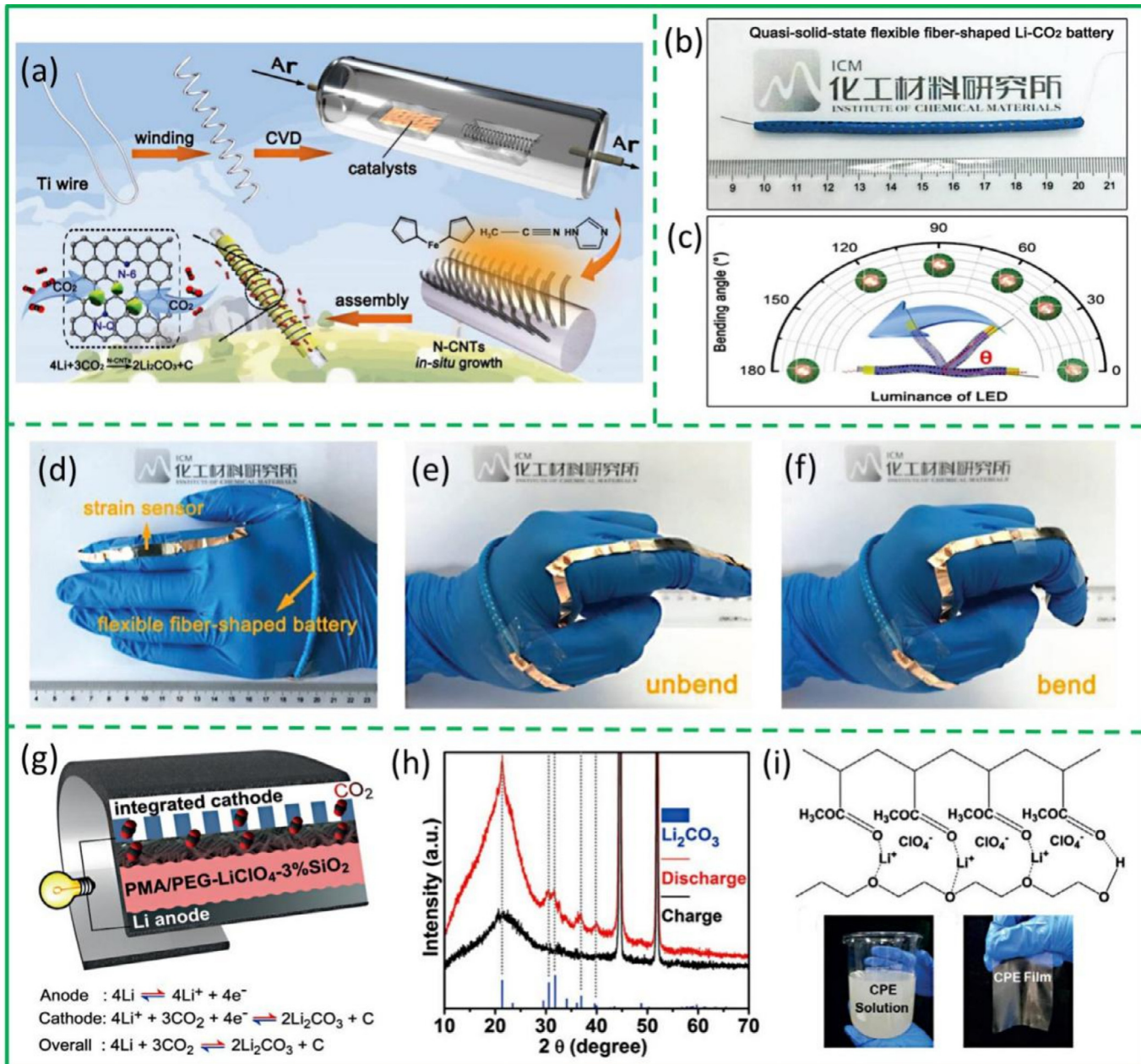


**Fig. 12.** (a) The synthesis process of N-CNTs@Ti electrode and the internal structure of the fabricated fiber-like device. (b) Photo of a quasi-solid flexible fibrous Li-CO<sub>2</sub> battery. (c) A 5 cm long fiber-shaped flexible Li-CO<sub>2</sub> battery, lighting a red LED at different bending angles. (d-f) Strain sensors based on CNT/PDMS hybrid membranes are powered by a 10 cm curved Li-CO<sub>2</sub> battery attached to a human's hand [111]. (g) All-solid-state Li-CO<sub>2</sub> battery with metal Li foil anode and CPE@CNTs cathode. (h) XRD pattern. (i) The molecular formula matrix of CPE, the solution and the CPE film on the CNTs cathode [216]. (For interpretation of the references to color in this figure legend, the reader is referred to the web version of this article.)

long fibrous Li-CO<sub>2</sub> battery to power a flexible strain sensor based on a CNT/polydimethylsiloxane (PDMS) hybrid membrane. The quasi-solid flexible fibrous Li-CO<sub>2</sub> battery can fit well on the irregular surface of humans' hand, and the strain sensor responds immediately when the fingers are repeatedly bent (Fig. 12d-f). These results reveal the huge potential of this quasi-solid flexible fibrous Li-CO<sub>2</sub> battery in practical applications, especially in wearable electronics.

In addition to GPE, another composite polymer electrolyte (CPE) has also attracted much attention. Chen et al. used polymethacrylate (PMA)/polyethylene glycol (PEG)-LiClO<sub>4</sub>-3 wt% SiO<sub>2</sub> liquid-free CPE for dye-sensitized solar and Li-ion batteries [214,215]. The organic-inorganic hybrid structure of this CPE is sticky and has a high ionic conductivity (0.26–0.57 ms cm<sup>-1</sup>). Later, the research group introduced

this CPE to a Li-CO<sub>2</sub> battery system [216]. The gelled and liquid-free CPE were directly coated on CNT material to form an integrated CPE@CNTs cathode structure, which avoids the use of adhesives, so that reduces the interface resistance. This flexible liquid-free Li-CO<sub>2</sub> battery configuration is shown in Fig. 12g. XRD characterization proves that the discharge product Li<sub>2</sub>CO<sub>3</sub> has a monoclinic phase and is easy to form and decompose (Fig. 12h). This non-transparent CPE solution was obtained by a one-pot reaction, and a translucent film was formed on the CNTs cathode by casting (Fig. 12i). This battery exhibits an extremely low overpotential (0.7 V) and stably cycles for 100 times at 558°C. Moreover, the large-scale production of flexible pouch-type Li-CO<sub>2</sub> battery has been realized. The battery has a reversible large capacity of 993.3 mAh g<sup>-1</sup>, a high energy density of 521 Wh kg<sup>-1</sup>, and can work for 220

hours under different bending degrees. The enhanced performance is attributed to the satisfactory ionic conductivity of CPE ( $7.14 \times 10^{-2}$  ms cm $^{-1}$ ) and mitigated interface resistance of the Li/CPE@CNTs cathode. This research provides a promising direction for the development of Li-CO<sub>2</sub> battery with higher power density, safety and mechanical flexibility. Two years later, Tao et al. prepared a composite solid electrolyte composed of polyethylene oxide (PEO) and 20 wt% Li<sub>7</sub>La<sub>3</sub>Zr<sub>1.4</sub>Ta<sub>0.6</sub>O<sub>12</sub> (LLZTO) for Li-CO<sub>2</sub> batteries [217]. The composite solid electrolyte has a high ionic conductivity ( $1.03 \times 10^{-3}$  S cm $^{-1}$  at 70°C), wide electrochemical window (5 V vs. Li $^{+}$ /Li), good mechanical properties and excellent flexibility. The Li symmetrical battery with PEO/LLZTO composite solid electrolyte can also work for 1500 hours at a current density of 0.1 mA cm $^{-1}$ . The assembled all-solid-state Li-CO<sub>2</sub> battery has a long cycle life of 70 cycles at a current density of 100 mA g $^{-1}$  and a fixed capacity of 1000 mAh g $^{-1}$ .

It is well known that the main problem facing solid electrolytes at present is the large impedance caused by solid-solid contact. Therefore, researchers have focused on gel-based solid electrolytes (add liquid electrolytes to the solid electrolytes) to improve the ionic conductivity, but still the problem of liquid electrolyte volatilization has remained unsolved. Thus, promising pure solid electrolytes are considered as the ultimate goal, which need to be further studied.

## 5. Conclusion and Outlook

The development and utilization of CO<sub>2</sub> gas play a vital role in solving global warming and energy shortage problems. Li-CO<sub>2</sub> battery, as a promising candidate, provides a new idea for capturing and utilizing CO<sub>2</sub>. However, the current development of Li-CO<sub>2</sub> battery is still in its initial stage and faces huge problems and challenges. Including high overpotential caused by wide band gap of Li<sub>2</sub>CO<sub>3</sub>, poor cycle performance, weak rate capability, low discharge capacity, etc. These problems are attributed to the slow reaction kinetics of CO<sub>2</sub> gas. Therefore, the development of efficient cathode catalysts and stable electrolytes are the first tasks to promote the electrochemical reaction of CO<sub>2</sub>. In this regard, this review provides a comprehensive overview of the electrochemical reaction mechanism of Li-CO<sub>2</sub> batteries and the latest design strategies for cathode catalysts and electrolytes. Although some advances have been made in previous research, there is still a long way to meet the all requirements for practical applications of Li-CO<sub>2</sub> batteries. Therefore, based on the analysis and discussion of the latest results, we explain some key dis-/advantages and future opportunities of Li-CO<sub>2</sub> batteries.

- (1) The charge-discharge mechanism of Li-CO<sub>2</sub> battery involves multiple interface reactions and complex electrochemical processes. The second chapter of this article reviews Li<sub>2</sub>CO<sub>3</sub>, C, Li<sub>2</sub>O, CO, Li<sub>2</sub>C<sub>2</sub>O<sub>4</sub> and other discharge products. Nonetheless, there are no current studies regarding the reason for existence of a variety of reaction products and the specific degradation of discharge products. Therefore, more research is needed to qualitatively and quantitatively analyze the CO<sub>2</sub> electrochemical reaction path. From the thermodynamic point of view, it is necessary to judge whether a chemical reaction can be formed, and calculate the formation energy and degradation energy of the reaction product to find the charge overpotential. From the kinetics point of view, it is necessary to determine the rate of electrochemical reaction, ion and electron transfer rate as well as oxidation-reduction reaction of the substance. By studying the charge-discharge reaction mechanism from these two aspects, it's believed that the electrochemical reaction process of Li-CO<sub>2</sub> batteries can be fully understood in the near future
- (2) The choice of cathode catalytic material plays a crucial role in Li-CO<sub>2</sub> electrochemistry. It has been mentioned that the chemical composition of the catalyst may affect the Li-CO<sub>2</sub> electrochemical performance, and different structures may affect CO<sub>2</sub>/Li $^{+}$  diffusion and discharge product deposition. However, more studies need to be car-

ried out to further explore the relationship between catalyst properties (space structure, defect effect, elemental composition, etc.) and electrochemical reactions, as well as the effect of discharge products on catalysts morphology. The primary issue is that the essence of the cathode catalyst has not been thoroughly understood so far. The catalysts' mechanism of effect and their function in redox reaction are still unknown. Thus, more in-depth research about the essence of catalysts has to be done in order to design a highly efficient Li-CO<sub>2</sub> battery catalyst.

- (3) The development of effective electrolytes is critical for Li-CO<sub>2</sub> battery systems in open environments. Multi-interface stability is the key for extending the service life of Li-CO<sub>2</sub> batteries. Although many studies have currently investigated different types of electrolytes, none of them has fully addressed the desired requirements so far. Moreover, the volatilization and leakage of liquid electrolytes in this open battery system cannot be avoided. Although applying additives can improve the electrochemical performance of the battery to some extent, there is no substantial evidence to prove the effect of additives on the electrochemical mechanism of Li-CO<sub>2</sub> batteries. Hence, more comprehensive investigation is required to find the most efficient and practical additive along with its mechanism of effect. On the other hand, solid electrolyte is a productive means to reduce electrolyte volatilization, and facilitate the development of wearable flexible batteries. Nevertheless, in an open environment, it is almost impossible to use a pure solid electrolyte, because the gas generation has a considerable effect on the interface, and consequently, the impedance will exponentially increase when there are bubbles on the interface. Therefore, in recent years, many efforts have been made to develop gel electrolytes, which still suffer from volatility. It is believed that to develop an effective electrolyte many factors need to be considered, including non-volatility, electrochemical stability, high conductivity, high ion mobility, and good compatibility with Li anode and CO<sub>2</sub> cathode. Achieving electrolytes with these characteristics is an appropriate strategy for realizing practical Li-CO<sub>2</sub> batteries.
- (4) The stability of Li metal anodes is another key part of Li-CO<sub>2</sub> batteries. Especially in the open system, many parasitic reactions will be triggered by factors such as H<sub>2</sub>O, O<sub>2</sub> mixing and the decomposition of electrolyte. Even if CO<sub>2</sub> gas can alleviate Li anode passivation and Li dendrite growth, these parasitic reactions are still inevitable and may cause large overpotential and sudden death of Li-CO<sub>2</sub> batteries. As mentioned above, the use of a liquid-free electrolyte is considered to be a method of protecting Li anodes. Additionally, constructing an artificial SEI film on the surface of Li metal is another solution to protect the Li-CO<sub>2</sub> anode. However, protective layer has to be stable, and not interfering with the entire electrochemical reaction. Accordingly, adding a protective layer involves the stability of multiple interfaces. Therefore, designing a stable and strong matrix is an effective approach to protect Li metal from adverse side reactions.

In summary, the rechargeable Li-CO<sub>2</sub> battery is an innovative device that realizes environmental protection. Despite all problems and challenges, we believe that through continuous efforts to develop efficient catalysts and stable electrolytes, and unraveling the charge-discharge reaction mechanism, practical Li-CO<sub>2</sub> batteries will be achieved in the future. Indeed, considering the current energy and environmental issues, it is expected that Li-CO<sub>2</sub> batteries will become the mainstream of the next-generation energy storage equipment.

## Author statement

All authors write the review article and proofread it.

## Declaration of Competing Interest

The authors declare no competing financial interest.

## Acknowledgements

This research was supported by the National Natural Science Foundation of China (51672189, 51801153, 51802261 and 52072298), Tianjin Science and Technology Project (18PTZWHZ00020), Natural Science Foundation of Shaanxi (2020JC-41), Project 2019JLP-04 supported by Joint Foundation of Shaanxi, Natural Science Foundation of Qinghai Province of China (2020-ZJ-910), and Xi'an Science and Technology Project of China (201805037YD15CG21(20)).

## References

- [1] J.M. Matter, M. Stute, S.O. Snaebjornsdottir, E.H. Oelkers, S.R. Gislason, E.S. Aradottir, B. Sigfusson, I. Gunnarsson, H. Sigurdardottir, E. Gunnlaugsson, G. Axelsson, H.A. Alfredsson, D. Wolffboenisch, K. Mesfin, D.F.D.L.R. Taya, J. Hall, K. Dideriksen, W.S. Broecker, Rapid carbon mineralization for permanent disposal of anthropogenic carbon dioxide emissions, *Science* 352 (2016) 1312–1314.
- [2] G.P. Peters, G. Marland, C. Le Quéré, T. Boden, J.G. Canadell, M.R. Raupach, Rapid growth in  $\text{CO}_2$  emissions after the 2008–2009 global financial crisis, *Nat. Clim. Change* 2 (2011) 2–4.
- [3] Y. Chen, C.W. Li, M.W. Kanan, Aqueous  $\text{CO}_2$  reduction at very low overpotential on oxide-derived Au nanoparticles, *J. Am. Chem. Soc.* 134 (2012) 19969–19972.
- [4] D.Y. Chung, S.W. Jun, G. Yoon, S.G. Kwon, D.Y. Shin, P. Seo, J.M. Yoo, H. Shin, Y.H. Chung, H. Kim, B.S. Mun, K.S. Lee, N.S. Lee, S.J. Yoo, D.H. Lim, K. Kang, Y.E. Sung, T. Hyeon, Highly durable and active PtFe nanocatalyst for electrochemical oxygen reduction reaction, *J. Am. Chem. Soc.* 137 (2015) 15478–15485.
- [5] W.I.A. Sadat, L.A. Archer, The  $\text{O}_2$ -assisted Al- $\text{CO}_2$  electrochemical cell-a system for  $\text{CO}_2$  capture conversion and electric power generation, *Sci. Adv.* 2 (2016) e1600968.
- [6] Z. Chang, J. Xu, X. Zhang, Recent progress in electrocatalyst for  $\text{Li}-\text{O}_2$  batteries, *Adv. Energy Mater.* 7 (2017) 1700875.
- [7] S. Chu, Y. Cui, N. Liu, The path towards sustainable energy, *Nat. Mater.* 16 (2016) 16–22.
- [8] Q. Zhao, X. Liu, S. Stalin, K. Khan, L.A. Archer, Solid-state polymer electrolytes with in-built fast interfacial transport for secondary lithium batteries, *Nat. Energy* 4 (2019) 365–373.
- [9] J.-c. Zheng, Z. Yang, Z.-j. He, H. Tong, W.-j. Yu, J.-f. Zhang, In situ formed  $\text{LiNi}_{0.8}\text{Co}_{0.15}\text{Al}_{0.05}\text{O}_2@\text{Li}_4\text{SiO}_4$  composite cathode material with high rate capability and long cycling stability for lithium-ion batteries, *Nano Energy* 53 (2018) 613–621.
- [10] M.A. Hannan, M.S.H. Lipu, A. Hussain, A. Mohamed, A review of lithium-ion battery state of charge estimation and management system in electric vehicle applications: challenges and recommendations, *Renewable Sustainable Energy Rev.* 78 (2017) 834–854.
- [11] S. Zheng, H. Xue, H. Pang, Supercapacitors based on metal coordination materials, *Coord. Chem. Rev.* 373 (2018) 2–21.
- [12] Y. Zhao, X. He, R. Chen, Q. Liu, J. Liu, J. Yu, J. Li, H. Zhang, H. Dong, M. Zhang, J. Wang, A flexible all-solid-state asymmetric supercapacitors based on hierarchical carbon cloth@ $\text{CoMoO}_4@\text{NiCo}$  layered double hydroxide core-shell heterostructures, *Chem. Eng. J.* 352 (2018) 29–38.
- [13] B. Kirubasankar, V. Murugadoss, J. Lin, T. Ding, M. Dong, H. Liu, J. Zhang, T. Li, N. Wang, Z. Guo, S. Angaiah, In situ grown nickel selenide on graphene nanohybrid electrodes for high energy density asymmetric supercapacitors, *Nanoscale* 10 (2018) 20414–20425.
- [14] Z.F. Pan, L. An, T.S. Zhao, Z.K. Tang, Advances and challenges in alkaline anion exchange membrane fuel cells, *Prog. Energy Combust. Sci.* 66 (2018) 141–175.
- [15] J. Wang, Y. Zhao, B.P. Setzler, S. Rojas-Carbonell, C. Ben Yehuda, A. Amel, M. Page, L. Wang, K. Hu, L. Shi, S. Gottesfeld, B. Xu, Y. Yan, Poly(aryl piperidinium) membranes and ionomers for hydroxide exchange membrane fuel cells, *Nat. Energy* 4 (2019) 392–398.
- [16] C. Wei, R.R. Rao, J. Peng, B. Huang, I.E.L. Stephens, M. Risch, Z.J. Xu, Y. Shao-Horn, Recommended practices and benchmark activity for hydrogen and oxygen electrocatalysis in water splitting and fuel cells, *Adv. Mater.* 31 (2019) e1806296.
- [17] M. Armand, J.-M. Tarascon, Building better batteries, *Nature* 451 (2008) 652–657.
- [18] T. Kim, W. Song, D.-Y. Son, L.K. Ono, Y. Qi, Lithium-ion batteries: outlook on present, future, and hybridized technologies, *J. Mater. Chem. A* 7 (2019) 2942–2964.
- [19] M.F. Lagadec, R. Zahn, V. Wood, Characterization and performance evaluation of lithium-ion battery separators, *Nat. Energy* 4 (2018) 16–25.
- [20] M. Winter, B. Barnett, K. Xu, Before Li ion batteries, *Chem. Rev.* 118 (2018) 11433–11456.
- [21] M. Li, J. Lu, Z. Chen, K. Amine, 30 Years of lithium-ion batteries, *Adv. Mater.* 30 (2018) 1800561.
- [22] H. Maleki Kheimeh Sari, X. Li, Controllable cathode–electrolyte interface of  $\text{Li}[\text{Ni}_{0.8}\text{Co}_{0.1}\text{Mn}_{0.1}]\text{O}_2$  for lithium ion batteries: a review, *Adv. Energy Mater.* 9 (2019) 1901597.
- [23] Q. Sun, J. Liu, B. Xiao, B. Wang, M. Banis, H. Yadegari, K.R. Adair, R. Li, X. Sun, Visualizing the oxidation mechanism and morphological evolution of the cubic-shaped superoxide discharge product in Na-air batteries, *Adv. Funct. Mater.* 29 (2019) 1808332.
- [24] S.S. Shinde, C.H. Lee, J.-Y. Jung, N.K. Wagh, S.-H. Kim, D.-H. Kim, C. Lin, S.U. Lee, J.-H. Lee, Unveiling dual-linkage 3D hexaiminobenzene metal–organic frameworks towards long-lasting advanced reversible Zn–air batteries, *Energy Environ. Sci.* 12 (2019) 727–738.
- [25] N. Xu, Y. Zhang, T. Zhang, Y. Liu, J. Qiao, Efficient quantum dots anchored nanocomposite for highly active ORR/OER electrocatalyst of advanced metal-air batteries, *Nano Energy* 57 (2019) 176–185.
- [26] Q. Sun, X. Lin, H. Yadegari, W. Xiao, Y. Zhao, K.R. Adair, R. Li, X. Sun, Aligning the binder effect on sodium–air batteries, *J. Mater. Chem. A* 6 (2018) 1473–1484.
- [27] D.U. Lee, P. Xu, Z.P. Cano, A.G. Kashkooli, M.G. Park, Z. Chen, Recent progress and perspectives on bi-functional oxygen electrocatalysts for advanced rechargeable metal–air batteries, *J. Mater. Chem. A* 4 (2016) 7107–7134.
- [28] Y. Li, J. Lu, Metal–Air Batteries, Will they be the future electrochemical energy storage device of choice? *ACS Energy Lett.* 2 (2017) 1370–1377.
- [29] M. Kim, H. Ju, J. Kim, Highly efficient bifunctional catalytic activity of bismuth rhodium oxide pyrochlore through tuning the covalent character for rechargeable aqueous Na-air batteries, *J. Mater. Chem. A* 6 (2018) 8523–8530.
- [30] B. Li, X. Ge, F.W. Goh, T.S. Hor, D. Geng, G. Du, Z. Liu, J. Zhang, X. Liu, Y. Zong,  $\text{Co}_3\text{O}_4$  nanoparticles decorated carbon nanofiber mat as binder-free air-cathode for high performance rechargeable zinc-air batteries, *Nanoscale* 7 (2015) 1830–1838.
- [31] Y. Huang, Y. Wang, C. Tang, J. Wang, Q. Zhang, Y. Wang, J. Zhang, Atomic modulation and structure design of carbons for bifunctional electrocatalysis in metal–air batteries, *Adv. Mater.* 31 (2019) e1803800.
- [32] H. Yadegari, M. Norouzi Banis, A. Lushington, Q. Sun, R. Li, T.-K. Sham, X. Sun, A bifunctional solid state catalyst with enhanced cycling stability for Na and  $\text{Li}-\text{O}_2$  cells: revealing the role of solid state catalysts, *Energy Environ. Sci.* 10 (2017) 286–295.
- [33] Q. Sun, H. Yadegari, M.N. Banis, J. Liu, B. Xiao, X. Li, C. Langford, R. Li, X. Sun, Toward a sodium–air battery: revealing the critical role of humidity, *J. Phys. Chem. C* 119 (2015) 13433–13441.
- [34] H. Yadegari, X. Sun, Sodium–oxygen batteries: recent developments and remaining challenges, *Trends Chem.* 2 (2020) 241–253.
- [35] C. Xu, K. Zhang, D. Zhang, S. Chang, F. Liang, P. Yan, Y. Yao, T. Qu, J. Zhan, W. Ma, B. Yang, Y. Dai, X. Sun, Reversible hybrid sodium– $\text{CO}_2$  batteries with low charging voltage and long-life, *Nano Energy* 68 (2020) 104318.
- [36] H. Yadegari, Q. Sun, X. Sun, Sodium–oxygen batteries: a comparative review from chemical and electrochemical fundamentals to future perspective, *Adv. Mater.* 28 (2016) 7065–7093.
- [37] H. Yadegari, M. Norouzi Banis, X. Lin, A. Koo, R. Li, X. Sun, Revealing the chemical mechanism of  $\text{NaO}_2$  decomposition by in situ Raman imaging, *Chem. Mater.* 30 (2018) 5156–5160.
- [38] H. Yadegari, X. Sun, Recent advances on sodium–oxygen batteries: a chemical perspective, *Acc. Chem. Res.* 51 (2018) 1532–1540.
- [39] M.N. Banis, H. Yadegari, Q. Sun, T. Regier, T. Boyko, J. Zhou, Y.M. Yiu, R. Li, Y. Hu, T.K. Sham, X. Sun, Revealing the charge/discharge mechanism of  $\text{Na}-\text{O}_2$  cells by in situ soft X-ray absorption spectroscopy, *Energy Environ. Sci.* 11 (2018) 2073–2077.
- [40] H. Yadegari, Y. Li, M.N. Banis, X. Li, B. Wang, Q. Sun, R. Li, T.-K. Sham, X. Cui, X. Sun, On rechargeability and reaction kinetics of sodium–air batteries, *Energy Environ. Sci.* 7 (2014) 3747–3757.
- [41] X. Lin, Q. Sun, H. Yadegari, X. Yang, Y. Zhao, C. Wang, J. Liang, A. Koo, R. Li, X. Sun, On the cycling performance of  $\text{Na}-\text{O}_2$  cells: revealing the impact of the superoxide crossover toward the metallic Na electrode, *Adv. Funct. Mater.* 28 (2018) 1801904.
- [42] F. Liang, X. Qiu, Q. Zhang, Y. Kang, A. Koo, K. Hayashi, K. Chen, D. Xue, K.N. Hui, H. Yadegari, X. Sun, A liquid anode for rechargeable sodium–air batteries with low voltage gap and high safety, *Nano Energy* 49 (2018) 574–579.
- [43] Y. Kang, F. Su, Q. Zhang, F. Liang, K.R. Adair, K. Chen, D. Xue, K. Hayashi, S.C. Cao, H. Yadegari, X. Sun, Novel high-energy-density rechargeable hybrid sodium–air cell with acidic electrolyte, *ACS Appl. Mater. Interfaces* 10 (2018) 23748–23756.
- [44] H. Yadegari, C.J. Franko, M.N. Banis, Q. Sun, R. Li, G.R. Goward, X. Sun, How to control the discharge products in  $\text{Na}-\text{O}_2$  cells: direct evidence toward the role of functional groups at the air electrode surface, *J. Phys. Chem. Lett.* 8 (2017) 4794–4800.
- [45] S. Han, C. Cai, F. Yang, Y. Zhu, Q. Sun, Y.G. Zhu, H. Li, H. Wang, Y. Shao-Horn, X. Sun, M. Gu, Interrogation of the reaction mechanism in a  $\text{Na}-\text{O}_2$  battery using in situ transmission electron microscopy, *ACS Nano* 14 (2020) 3669–3677.
- [46] Z.E. Reeve, C.J. Franko, K.J. Harris, H. Yadegari, X. Sun, G.R. Goward, Detection of electrochemical reaction products from the sodium–oxygen cell with solid-state (23)Na NMR spectroscopy, *J. Am. Chem. Soc.* 139 (2017) 595–598.
- [47] X. Lin, J. Wang, X. Gao, S. Wang, Q. Sun, J. Luo, C. Zhao, Y. Zhao, X. Yang, C. Wang, R. Li, X. Sun, 3D printing of free-standing “ $\text{O}_2$  breathable” air electrodes for high-capacity and long-life  $\text{Na}-\text{O}_2$  batteries, *Chem. Mater.* 32 (2020) 3018–3027.
- [48] P. Tan, Z.H. Wei, W. Shyy, T.S. Zhao, X.B. Zhu, A nano-structured  $\text{RuO}_2/\text{NiO}$  cathode enables the operation of non-aqueous lithium–air batteries in ambient air, *Energy Environ. Sci.* 9 (2016) 1783–1793.
- [49] D. Aurbach, B.D. McCloskey, L.F. Nazar, P.G. Bruce, Advances in understanding mechanisms underpinning lithium–air batteries, *Nat. Energy* 1 (2016) 16128.
- [50] D. Geng, N. Ding, T.S.A. Hor, S.W. Chien, Z. Liu, D. Wuu, X. Sun, Y. Zong, From lithium–oxygen to lithium–air batteries: challenges and opportunities, *Adv. Energy Mater.* 6 (2016) 1502164.
- [51] J. Wang, Y. Li, X. Sun, Challenges and opportunities of nanostructured materials for aprotic rechargeable lithium–air batteries, *Nano Energy* 2 (2013) 443–467.
- [52] A.C. Luntz, B.D. McCloskey, Nonaqueous Li–air batteries: a status report, *Chem. Rev.* 114 (2014) 11721–11750.
- [53] A. Dutta, K. Ito, Y. Kubo, Establishing the criteria and strategies to achieve high power during discharge of a Li–air battery, *J. Mater. Chem. A* 7 (2019) 23199–23207.

- [54] J.B. Park, S.H. Lee, H.G. Jung, D. Aurbach, Y.K. Sun, Redox mediators for Li-O<sub>2</sub> batteries: status and perspectives, *Adv. Mater.* (2018) 30.
- [55] V. Giordani, D. Tozier, H. Tan, C.M. Burke, B.M. Gallant, J. Uddin, J.R. Greer, B.D. McCloskey, G.V. Chase, D. Addison, A molten salt lithium-oxygen battery, *J. Am. Chem. Soc.* 138 (2016) 2656–2663.
- [56] C. Xia, C.Y. Kwok, L.F. Nazar, A high-energy-density lithium-oxygen battery based on a reversible four-electron conversion to lithium oxide, *Science* 361 (2018) 777–781.
- [57] C. Zhao, C. Yu, S. Li, W. Guo, Y. Zhao, Q. Dong, X. Lin, Z. Song, X. Tan, C. Wang, M. Zheng, X. Sun, J. Qiu, Ultrahigh-capacity and long-life lithium-metal batteries enabled by engineering carbon nanofiber-stabilized graphene aerogel film host, *Small* 14 (2018) e1803310.
- [58] Y. Sun, M. Amirmaleki, Y. Zhao, C. Zhao, J. Liang, C. Wang, K.R. Adair, J. Li, T. Cui, G. Wang, R. Li, T. Filletter, M. Cai, T.K. Sham, X. Sun, Tailoring the mechanical and electrochemical properties of an artificial interphase for high-performance metallic lithium anode, *Adv. Energy Mater.* 10 (2020) 2001139.
- [59] Y. Li, J. Wang, X. Li, D. Geng, R. Li, X. Sun, Superior energy capacity of graphene nanosheets for a nonaqueous lithium-oxygen battery, *Chem. Commun. (Camb.)* 47 (2011) 9438–9440.
- [60] K.R. Adair, C. Zhao, M.N. Banis, Y. Zhao, R. Li, M. Cai, X. Sun, Highly stable lithium metal anode interface via molecular layer deposition zirconia coatings for long life next-generation battery systems, *Angew. Chem. Int. Ed. Engl.* 58 (2019) 15797–15802.
- [61] S.R. Gowda, A. Brunet, G.M. Wallraff, B.D. McCloskey, Implications of CO<sub>2</sub> contamination in rechargeable nonaqueous Li-O<sub>2</sub> batteries, *J. Phys. Chem. Lett.* 4 (2013) 276–279.
- [62] S. Meini, N. Tsouvaras, K.U. Schwenke, M. Piana, H. Beyer, L. Lange, H.A. Gasteiger, Rechargeability of Li-air cathodes pre-filled with discharge products using an ether-based electrolyte solution: implications for cycle-life of Li-air cells, *Phys. Chem. Chem. Phys.* 15 (2013) 11478–11493.
- [63] X.B. Zhu, T.S. Zhao, Z.H. Wei, P. Tan, L. An, A high-rate and long cycle life solid-state lithium-air battery, *Energy Environ. Sci.* 8 (2015) 3745–3754.
- [64] Y. Shen, D. Sun, L. Yu, W. Zhang, Y. Shang, H. Tang, J. Wu, A. Cao, Y. Huang, A high-capacity lithium-air battery with Pd modified carbon nanotube sponge cathode working in regular air, *Carbon* 62 (2013) 288–295.
- [65] H.D. Lim, B. Lee, Y. Bae, H. Park, Y. Ko, H. Kim, J. Kim, K. Kang, Reaction chemistry in rechargeable Li-O<sub>2</sub> batteries, *Chem. Soc. Rev.* 46 (2017) 2873–2888.
- [66] Y. Qiao, J. Yi, S. Guo, Y. Sun, S. Wu, X. Liu, S. Yang, P. He, H. Zhou, Li<sub>2</sub>CO<sub>3</sub>-free Li-O<sub>2</sub>/CO<sub>2</sub> battery with peroxide discharge product, *Energy Environ. Sci.* 11 (2018) 1211–1217.
- [67] F. Marques Mota, J.H. Kang, Y. Jung, J. Park, M. Na, D.H. Kim, H.R. Byon, Mechanistic study revealing the role of the Br<sup>3-</sup>/Br<sub>2</sub> redox couple in CO<sub>2</sub> assisted Li-O<sub>2</sub> batteries, *Adv. Energy Mater.* 10 (2020) 1903486.
- [68] K. Takechi, T. Shiga, T. Asaoka, A Li-O<sub>2</sub>/CO<sub>2</sub> battery, *Chem. Commun. (Camb.)* 47 (2011) 3463–3465.
- [69] B. Huang, G. Frapper, Pressure-induced polymerization of CO<sub>2</sub> in lithium-carbon dioxide phases, *J. Am. Chem. Soc.* 140 (2018) 413–422.
- [70] M. Goodarzi, F. Nazari, F. Illas, Assessing the performance of cobalt phthalocyanine nanoflakes as molecular catalysts for Li-promoted oxalate formation in Li-CO<sub>2</sub>-oxalate batteries, *J. Phys. Chem. C* 122 (2018) 25776–25784.
- [71] X. Xiao, W. Shang, W. Yu, Y. Ma, P. Tan, B. Chen, W. Kong, H. Xu, M. Ni, Toward the rational design of cathode and electrolyte materials for aprotic Li-CO<sub>2</sub> batteries: a numerical investigation, *Int. J. Energy Res.* 44 (2019) 496–507.
- [72] B. Liu, Y. Sun, L. Liu, J. Chen, B. Yang, S. Xu, X. Yan, Recent advances in understanding Li-CO<sub>2</sub> electrochemistry, *Energy Environ. Sci.* 12 (2019) 887–922.
- [73] Y. Mao, C. Tang, Z. Tang, J. Xie, Z. Chen, J. Tu, G. Cao, X. Zhao, Long-life Li-CO<sub>2</sub> cells with ultrafine IrO<sub>2</sub> decorated few-layered δ-MnO<sub>2</sub> enabling amorphous Li<sub>2</sub>CO<sub>3</sub> growth, *Energy Storage Mater.* 18 (2019) 405–413.
- [74] L. Song, T. Wang, C. Wu, X. Fan, J. He, A long-life Li-CO<sub>2</sub> battery employing a cathode catalyst of cobalt-embedded nitrogen-doped carbon nanotubes derived from a Prussian blue analogue, *Chem. Commun. (Camb.)* 55 (2019) 12781–12784.
- [75] S. Xu, S.K. Das, L.A. Archer, The Li-CO<sub>2</sub> battery: a novel method for CO<sub>2</sub> capture and utilization, *RSC Adv.* 3 (2013) 6656.
- [76] A. Hu, C. Shu, C. Xu, R. Liang, J. Li, R. Zheng, M. Li, J. Long, Design strategies toward catalytic materials and cathode structures for emerging Li-CO<sub>2</sub> batteries, *J. Mater. Chem. A* 7 (2019) 21605–21633.
- [77] X. Li, J. Zhou, J. Zhang, M. Li, X. Bi, T. Liu, T. He, J. Cheng, F. Zhang, Y. Li, X. Mu, J. Lu, B. Wang, Bamboo-like nitrogen-doped carbon nanotube forests as durable metal-free catalysts for self-powered flexible Li-CO<sub>2</sub> batteries, *Adv. Mater.* 31 (2019) e1903852.
- [78] H. Liang, Y. Zhang, F. Chen, S. Jing, S. Yin, P. Tsakarais, A novel NiFe@NC-functionalized N-doped carbon microtubule network derived from biomass as a highly efficient 3D free-standing cathode for Li-CO<sub>2</sub> batteries, *Appl. Catal. B* 244 (2019) 559–567.
- [79] L. Wang, W. Dai, L. Ma, L. Gong, Z. Lyu, Y. Zhou, J. Liu, M. Lin, M. Lai, Z. Peng, W. Chen, Monodispersed Ru nanoparticles functionalized graphene nanosheets as efficient cathode catalysts for O<sub>2</sub>-assisted Li-CO<sub>2</sub> battery, *ACS Omega* 2 (2017) 9280–9286.
- [80] Y. Liu, R. Wang, Y. Lyu, H. Li, L. Chen, Rechargeable Li/CO-O (2:1) battery and Li/CO<sub>2</sub> battery, *Energy Environ. Sci.* 7 (2014) 677.
- [81] Z. Zhang, Q. Zhang, Y. Chen, J. Bao, X. Zhou, Z. Xie, J. Wei, Z. Zhou, The first introduction of graphene to rechargeable Li-CO<sub>2</sub> batteries, *Angew. Chem. Int. Ed. Engl.* 54 (2015) 6550–6553.
- [82] X. Zhang, Q. Zhang, Z. Zhang, Y. Chen, Z. Xie, J. Wei, Z. Zhou, Rechargeable Li-CO<sub>2</sub> batteries with carbon nanotubes as air cathodes, *Chem. Commun.* 51 (2015) 14636–14639.
- [83] Y. Qiao, J. Yi, S. Wu, Y. Liu, S. Yang, P. He, H. Zhou, Li-CO<sub>2</sub> electrochemistry: a new strategy for CO<sub>2</sub> fixation and energy storage, *Joule* 1 (2017) 359–370.
- [84] Z. Peng, S.A. Freunberger, Y. Chen, P.G. Bruce, A reversible and higher-rate Li-O<sub>2</sub> battery, *Science* 337 (2012) 563–566.
- [85] G.H. Lee, S. Lee, J.C. Kim, D.W. Kim, Y. Kang, D.W. Kim, MnMoO<sub>4</sub> electrocatalysts for superior long-life and high-rate lithium oxygen batteries, *Adv. Energy Mater.* 7 (2016) 1601741.
- [86] Y. Jing, Z. Zhou, Computational Insights into oxygen reduction reaction and initial Li<sub>2</sub>O<sub>2</sub> nucleation on pristine and N-doped graphene in Li-O<sub>2</sub> batteries, *ACS Catal.* 5 (2015) 4309–4317.
- [87] J. Lu, L. Li, J.B. Park, Y.K. Sun, F. Wu, K. Armine, Aprotic and aqueous Li-O(2) batteries, *Chem. Rev.* 114 (2014) 5611–5640.
- [88] Y. Hou, J. Wang, L. Liu, Y. Liu, S. Chou, D. Shi, H. Liu, Y. Wu, W. Zhang, J. Chen, MoC/CNT: an efficient catalyst for rechargeable Li-CO<sub>2</sub> batteries, *Adv. Funct. Mater.* 27 (2017) 1700564.
- [89] S. Yang, P. He, H. Zhou, Exploring the electrochemical reaction mechanism of carbonate oxidation in Li-air/CO<sub>2</sub> battery through tracing missing oxygen, *Energy Environ. Sci.* 9 (2016) 1650–1654.
- [90] S. Yang, Y. Qiao, P. He, Y. Liu, Z. Cheng, J.-j. Zhu, H. Zhou, A reversible lithium-CO<sub>2</sub> battery with Ru nanoparticles as a cathode catalyst, *Energy Environ. Sci.* 10 (2017) 972–978.
- [91] S. Li, Y. Liu, J. Zhou, S. Hong, Y. Dong, J. Wang, X. Gao, P. Qi, Y. Han, B. Wang, Monodispersed MnO nanoparticles in graphene-an interconnected N-doped 3D carbon framework as a highly efficient gas cathode in Li-CO<sub>2</sub> batteries, *Energy Environ. Sci.* 12 (2019) 1046–1054.
- [92] Z. Zhang, X.G. Wang, X. Zhang, Z. Xie, Y.N. Chen, L. Ma, Z. Peng, Z. Zhou, Verifying the rechargeability of Li-CO<sub>2</sub> batteries on working cathodes of Ni nanoparticles highly dispersed on N-doped graphene, *Adv. Sci. (Weinh.)* 5 (2018) 1700567.
- [93] A. Ahmadiparidari, R.E. Warburton, L. Majidi, M. Asadi, A. Chamaani, J.R. Jokisaari, S. Rastegar, Z. Hemmat, B. Sayahpour, R.S. Assary, B. Narayanan, P. Abbasi, P.C. Redfern, A. Ngo, M. Voros, J. Greeley, R. Klle, L.A. Curtiss, A. Salehi-Khojin, A long-cycle-life lithium-CO<sub>2</sub> battery with carbon neutrality, *Adv. Mater.* 31 (2019) e1902518.
- [94] Y. Xing, Y. Yang, D. Li, M. Luo, N. Chen, Y. Ye, J. Qian, L. Li, D. Yang, F. Wu, R. Chen, S. Guo, Crumpled Ir nanosheets fully covered on porous carbon nanofibers for long-life rechargeable lithium-CO<sub>2</sub> batteries, *Adv. Mater.* 30 (2018) e1803124.
- [95] J. Zhou, X. Li, C. Yang, Y. Li, K. Guo, J. Cheng, D. Yuan, C. Song, J. Lu, B. Wang, A quasi-solid-state flexible fiber-shaped Li-CO<sub>2</sub> battery with low overpotential and high energy efficiency, *Adv. Mater.* 31 (2019) e1804439.
- [96] J.H. Montoya, L.C. Seitz, P. Chakrhanont, A. Vojvodic, T.F. Jaramillo, J.K. Norskov, Materials for solar fuels and chemicals, *Nat. Mater.* 16 (2016) 70–81.
- [97] J. Xie, Q. Liu, Y. Huang, M. Wu, Y. Wang, A porous Zn cathode for Li-CO<sub>2</sub> batteries generating fuel-gas CO, *J. Mater. Chem. A* 6 (2018) 13952–13958.
- [98] X. Zhang, Q. Zhang, Z. Zhang, Y. Chen, Z. Xie, J. Wei, Z. Zhou, Rechargeable Li-CO<sub>2</sub> batteries with carbon nanotubes as air cathodes, *Chem. Commun. (Camb.)* 51 (2015) 14636–14639.
- [99] J. Li, H. Zhao, H. Qi, X. Sun, X. Song, Z. Guo, A.G. Tamirat, J. Liu, L. Wang, S. Feng, Drawing a pencil-trace cathode for a high performance polymer-based Li-CO<sub>2</sub> battery with redox mediator, *Adv. Funct. Mater.* 29 (2019) 1806863.
- [100] W. Xing, S. Li, D. Du, D. Wang, Y. Liao, S. Ge, J. Xu, P. Bai, Z. Liu, Y. Wang, X. Gao, M. Wu, Q. Xue, Z. Yan, Revealing the impacting factors of cathodic carbon catalysts for Li-CO<sub>2</sub> batteries in the pore-structure point of view, *Electrochim. Acta* 311 (2019) 41–49.
- [101] Y. Li, J. Wang, X. Li, D. Geng, M.N. Banis, Y. Tang, D. Wang, R. Li, T.-K. Sham, X. Sun, Discharge product morphology and increased charge performance of lithium–oxygen batteries with graphene nanosheet electrodes: the effect of sulphur doping, *J. Mater. Chem. A* 22 (2012) 20170.
- [102] Y. Li, J. Wang, X. Li, D. Geng, M.N. Banis, R. Li, X. Sun, Nitrogen-doped graphene nanosheets as cathode materials with excellent electrocatalytic activity for high capacity lithium–oxygen batteries, *Electrochim. Commun.* 18 (2012) 12–15.
- [103] Y. Li, J. Wang, X. Li, J. Liu, D. Geng, J. Yang, R. Li, X. Sun, Nitrogen-doped carbon nanotubes as cathode for lithium–air batteries, *Electrochim. Commun.* 13 (2011) 668–672.
- [104] C. Zhao, Z. Wang, X. Tan, H. Huang, Z. Song, Y. Sun, S. Cui, Q. Wei, W. Guo, R. Li, C. Yu, J. Qiu, X. Sun, Implanting CNT forest onto carbon nanosheets as multifunctional hosts for high-performance lithium metal batteries, *Small Methods* 3 (2019) 1800546.
- [105] Q. Sun, H. Yadegari, M.N. Banis, J. Liu, B. Xiao, B. Wang, S. Lawes, X. Li, R. Li, X. Sun, Self-stacked nitrogen-doped carbon nanotubes as long-life air electrode for sodium-air batteries: elucidating the evolution of discharge product morphology, *Nano Energy* 12 (2015) 698–708.
- [106] Q. Lv, W. Si, J. He, L. Sun, C. Zhang, N. Wang, Z. Yang, X. Li, X. Wang, W. Deng, Y. Long, C. Huang, Y. Li, Selectively nitrogen-doped carbon materials as superior metal-free catalysts for oxygen reduction, *Nat. Commun.* 9 (2018) 3376.
- [107] C.H. Lin, H.L. Chang, C.M. Hsu, A.Y. Lo, C.T. Kuo, The role of nitrogen in carbon nanotube formation, *Diam. Relat. Mater.* 12 (2003) 1851–1857.
- [108] H. Jiang, J. Gu, X. Zheng, M. Liu, X. Qiu, L. Wang, W. Li, Z. Chen, X. Ji, J. Li, Defect-rich and ultrathin N doped carbon nanosheets as advanced trifunctional metal-free electrocatalysts for the ORR, OER and HER, *Energy Environ. Sci.* 12 (2019) 322–333.
- [109] H. Yadegari, M.N. Banis, B. Xiao, Q. Sun, X. Li, A. Lushington, B. Wang, R. Li, T.-K. Sham, X. Cui, X. Sun, Three-dimensional nanostructured air electrode for sodium–oxygen batteries: a mechanism study toward the cyclability of the cell, *Chem. Mater.* 27 (2015) 3040–3047.

- [110] Y. Li, H. Yadegari, X. Li, M.N. Banis, R. Li, X. Sun, Superior catalytic activity of nitrogen-doped graphene cathodes for high energy capacity sodium-air batteries, *Chem. Commun. (Camb.)* 49 (2013) 11731–11733.
- [111] Y. Li, J. Zhou, T. Zhang, T. Wang, X. Li, Y. Jia, J. Cheng, Q. Guan, E. Liu, H. Peng, B. Wang, Highly surface-wrinkled and N-doped CNTs anchored on metal wire: a novel fiber-shaped cathode toward high-performance flexible Li–CO<sub>2</sub> batteries, *Adv. Funct. Mater.* 29 (2019) 1808117.
- [112] L. Qie, Y. Lin, J. Connell, J. Xu, L. Dai, Highly rechargeable lithium–CO<sub>2</sub> batteries with a boron and nitrogen-codoped holey-graphene cathode, *Angew. Chem.* 56 (2017) 6970–6974.
- [113] B.W. Zhang, Y. Jiao, D.L. Chao, C. Ye, Y.X. Wang, K. Davey, H.K. Liu, S.X. Dou, S.Z. Qiao, Targeted synergy between adjacent co atoms on graphene oxide as an efficient new electrocatalyst for Li–CO<sub>2</sub> batteries, *Adv. Funct. Mater.* 29 (2019) 1904206.
- [114] A. Shen, Y. Zou, Q. Wang, R.A. Dryfe, X. Huang, S. Dou, L. Dai, S. Wang, Oxygen reduction reaction in a droplet on graphite: direct evidence that the edge is more active than the basal plane, *Angew. Chem. Int. Ed. Engl.* 53 (2014) 10804–10808.
- [115] H. Jin, H. Huang, Y. He, X. Feng, S. Wang, L. Dai, J. Wang, Graphene quantum dots supported by graphene nanoribbons with ultrahigh electrocatalytic performance for oxygen reduction, *J. Am. Chem. Soc.* 137 (2015) 7588–7591.
- [116] S.Y. Lim, W. Shen, Z. Gao, Carbon quantum dots and their applications, *Chem. Soc. Rev.* 44 (2015) 362–381.
- [117] Y. Jin, C. Hu, Q. Dai, Y. Xiao, Y. Lin, J.W. Connell, F. Chen, L. Dai, High-performance Li–CO<sub>2</sub> batteries based on metal-free carbon quantum dot/holey graphene composite catalysts, *Adv. Funct. Mater.* 28 (2018) 1804630.
- [118] J. Kim, H.E. Kim, H. Lee, Single-atom catalysts of precious metals for electrochemical reactions, *ChemSusChem* 11 (2018) 104–113.
- [119] Q. Shi, C. Zhu, D. Du, Y. Lin, Robust noble metal-based electrocatalysts for oxygen evolution reaction, *Chem. Soc. Rev.* 48 (2019) 3181–3192.
- [120] B. Sun, S. Chen, H. Liu, G. Wang, Mesoporous carbon nanocube architecture for high-performance lithium–oxygen batteries, *Adv. Funct. Mater.* 25 (2015) 4436–4444.
- [121] B. Sun, X. Huang, S. Chen, P. Munroe, G. Wang, Porous graphene nanoarchitectures: an efficient catalyst for low charge-overpotential, long life, and high capacity lithium–oxygen batteries, *Nano Lett.* 14 (2014) 3145–3152.
- [122] D. Su, D. Han Seo, Y. Ju, Z. Han, K. Ostrikov, S. Dou, H.-J. Ahn, Z. Peng, G. Wang, Ruthenium nanocrystal decorated vertical graphene nanosheets@Ni foam as highly efficient cathode catalysts for lithium–oxygen batteries, *NPG Asia Mater.* 8 (2016) e286–e286.
- [123] H. Jung, Y.S. Jeong, J. Park, Y. Sun, B. Scrosati, Y.J. Lee, Ruthenium-based electrocatalysts supported on reduced graphene oxide for lithium–air batteries, *ACS Nano* 7 (2013) 3532–3539.
- [124] C. Zhao, C. Yu, M.N. Banis, Q. Sun, M. Zhang, X. Li, Y. Liu, Y. Zhao, H. Huang, S. Li, X. Han, B. Xiao, Z. Song, R. Li, J. Qiu, X. Sun, Decoupling atomic-layer-deposition ultrafine RuO<sub>2</sub> for high-efficiency and ultralong-life Li–O<sub>2</sub> batteries, *Nano Energy* 34 (2017) 399–407.
- [125] J.J. Xu, Z.L. Wang, D. Xu, L.L. Zhang, X.B. Zhang, Tailoring deposition and morphology of discharge products towards high-rate and long-life lithium–oxygen batteries, *Nat. Commun.* 4 (2013) 2438.
- [126] Z. Zhang, C. Yang, S. Wu, A. Wang, L. Zhao, D. Zhai, B. Ren, K. Cao, Z. Zhou, Exploiting synergistic effect by integrating ruthenium–copper nanoparticles highly co-dispersed on graphene as efficient air cathodes for Li–CO<sub>2</sub> batteries, *Adv. Energy Mater.* 9 (2019) 1802805.
- [127] H. Zhao, D. Li, H. Li, A.G. Tamirat, X. Song, Z. Zhang, Y. Wang, Z. Guo, L. Wang, S. Feng, Ru nanosheet catalyst supported by three-dimensional nickel foam as a binder-free cathode for Li–CO<sub>2</sub> batteries, *Electrochim. Acta* 299 (2019) 592–599.
- [128] Y. Qiao, S. Xu, Y. Liu, J. Dai, H. Xie, Y. Yao, X. Mu, C. Chen, D.J. Kline, E.M. Hitz, B. Liu, J. Song, P. He, M.R. Zachariah, L. Hu, Transient, *in situ* synthesis of ultrafine ruthenium nanoparticles for a high-rate Li–CO<sub>2</sub> battery, *Energy Environ. Sci.* 12 (2019) 1100–1107.
- [129] S. Bie, M. Du, W. He, H. Zhang, Z. Yu, J. Liu, M. Liu, W. Yan, L. Zhou, Z. Zou, Carbon nanotube@RuO<sub>2</sub> as a high performance catalyst for Li–CO<sub>2</sub> batteries, *ACS Appl. Mater. Interfaces* 11 (2019) 5146–5151.
- [130] Z. Guo, J. Li, H. Qi, X. Sun, H. Li, A.G. Tamirat, J. Liu, Y. Wang, L. Wang, A highly reversible long-life Li–CO<sub>2</sub> battery with a RuP<sub>2</sub><sup>-</sup>-based catalytic cathode, *Small* 15 (2019) e1803246.
- [131] Q. Cheng, H.F. Tu, C. Zheng, J.P. Qu, G. Helmchen, S.L. You, Iridium-catalyzed asymmetric allylic substitution reactions, *Chem. Rev.* 119 (2019) 1855–1969.
- [132] Y. Zhang, C. Wu, H. Jiang, Y. Lin, H. Liu, Q. He, S. Chen, T. Duan, L. Song, Atomic iridium incorporated in cobalt hydroxide for efficient oxygen evolution catalysis in neutral electrolyte, *Adv. Mater.* 30 (2018) e1707522.
- [133] Y. Pi, N. Zhang, S. Guo, J. Guo, X. Huang, Ultrathin laminar Ir superstructure as highly efficient oxygen evolution electrocatalyst in broad pH range, *Nano Lett.* 16 (2016) 4424–4430.
- [134] J. Lu, Y.J. Lee, X. Luo, K.C. Lau, M. Asadi, H.H. Wang, S. Brombosz, J. Wen, D. Zhai, Z. Chen, D.J. Miller, Y.S. Jeong, J.B. Park, Z.Z. Fang, B. Kumar, A. Salehi-Khojin, Y.K. Sun, L.A. Curtiss, K. Amine, A lithium–oxygen battery based on lithium superoxide, *Nature* 529 (2016) 377–382.
- [135] S. Song, W. Xu, J. Zheng, L. Luo, M.H. Engelhard, M.E. Bowden, B. Liu, C.M. Wang, J.G. Zhang, Complete decomposition of Li<sub>2</sub>CO<sub>3</sub> in Li–O<sub>2</sub> batteries using Ir/B<sub>4</sub>C as noncarbon-based oxygen electrode, *Nano Lett.* 17 (2017) 1417–1424.
- [136] C. Wang, Q. Zhang, X. Zhang, X.G. Wang, Z. Xie, Z. Zhou, Fabricating Ir/C nanofiber networks as free-standing air cathodes for rechargeable Li–CO<sub>2</sub> batteries, *Small* 14 (2018) e1800641.
- [137] W. Zhao, X. Li, R. Yin, L. Qian, X. Huang, H. Liu, J. Zhang, J. Wang, T. Ding, Z. Guo, Urchin-like NiO–NiCo<sub>2</sub>O<sub>4</sub> heterostructure microsphere catalysts for enhanced rechargeable non-aqueous Li–O<sub>2</sub> batteries, *Nanoscale* 11 (2018) 50–59.
- [138] H. Wang, H. Wang, J. Huang, X. Zhou, Q. Wu, Z. Luo, F. Wang, Hierarchical mesoporous/macroporous co-doped NiO nanosheet arrays as free-standing electrode materials for rechargeable Li–O<sub>2</sub> batteries, *ACS Appl. Mater. Interfaces* 11 (2019) 44556–44565.
- [139] J. Long, Z. Hou, C. Shu, C. Han, W. Li, R. Huang, J. Wang, Free-standing three-dimensional CuCo<sub>2</sub>S<sub>4</sub> nanosheet array with high catalytic activity as an efficient oxygen electrode for lithium–oxygen batteries, *ACS Appl. Mater. Interfaces* 11 (2019) 3834–3842.
- [140] Q.C. Liu, J.J. Xu, D. Xu, X.B. Zhang, Flexible lithium–oxygen battery based on a recoverable cathode, *Nat. Commun.* 6 (2015) 7892.
- [141] J.J. Xu, D. Xu, Z.L. Wang, H.G. Wang, L.L. Zhang, X.B. Zhang, Synthesis of perovskite-based porous La<sub>0.75</sub>Sr<sub>0.25</sub>MnO<sub>3</sub> nanotubes as a highly efficient electrocatalyst for rechargeable lithium–oxygen batteries, *Angew. Chem. Int. Ed. Engl.* 52 (2013) 3887–3890.
- [142] Q. Liu, Y. Jiang, J. Xu, D. Xu, Z. Chang, Y. Yin, W. Liu, X. Zhang, Hierarchical Co<sub>3</sub>O<sub>4</sub> porous nanowires as an efficient bifunctional cathode catalyst for long life Li–O<sub>2</sub> batteries, *Nano Res.* 8 (2014) 576–583.
- [143] X. Sun, L. Lu, Q. Zhu, C. Wu, D. Yang, C. Chen, B. Han, MoP nanoparticles supported on indium-doped porous carbon: outstanding catalysts for highly efficient CO<sub>2</sub> electroreduction, *Angew. Chem. Int. Ed. Engl.* 57 (2018) 2427–2431.
- [144] F. Cheng, T. Zhang, Y. Zhang, J. Du, X. Han, J. Chen, Enhancing electrocatalytic oxygen reduction on MnO(2) with vacancies, *Angew. Chem. Int. Ed. Engl.* 52 (2013) 2474–2477.
- [145] Y. Jin, F. Chen, J. Wang, R.L. Johnston, Tuning electronic and composition effects in ruthenium–copper alloy nanoparticles anchored on carbon nanofibers for rechargeable Li–CO<sub>2</sub> batteries, *Chem. Eng. J.* 375 (2019) 121978.
- [146] Z. Zhang, Z. Zhang, P. Liu, Y. Xie, K. Cao, Z. Zhou, Identification of cathode stability in Li–CO<sub>2</sub> batteries with Cu nanoparticles highly dispersed on N-doped graphene, *J. Mater. Chem. A* 6 (2018) 3218–3223.
- [147] Y. Qiao, Y. Liu, C. Chen, H. Xie, Y. Yao, S. He, W. Ping, B. Liu, L. Hu, 3D-printed graphene oxide framework with thermal shock synthesized nanoparticles for Li–CO<sub>2</sub> batteries, *Adv. Funct. Mater.* 28 (2018) 1805899.
- [148] K. Huang, Y. Sun, Y. Zhang, X. Wang, W. Zhang, S. Feng, Hollow-structured metal oxides as oxygen-related catalysts, *Adv. Mater.* 31 (2019) e1801430.
- [149] R. Wang, X. Yu, J. Bai, H. Li, X. Huang, L. Chen, X. Yang, Electrochemical decomposition of Li<sub>2</sub>CO<sub>3</sub> in NiO–Li<sub>2</sub>CO<sub>3</sub> nanocomposite thin film and powder electrodes, *J. Power Sources* 218 (2012) 1113–1118.
- [150] M. Hong, H.C. Choi, H.R. Byon, Nanoporous NiO plates with a unique role for promoted oxidation of carbonate and carboxylate species in the Li–O<sub>2</sub> battery, *Chem. Mater.* 27 (2015) 2234–2241.
- [151] X. Zhang, C. Wang, H. Li, X.-G. Wang, Y.-N. Chen, Z. Xie, Z. Zhou, High performance Li–CO<sub>2</sub> batteries with NiO–CNT cathodes, *J. Mater. Chem. A* 6 (2018) 2792–2796.
- [152] S. Lu, Y. Shang, S. Ma, Y. Lu, Q.C. Liu, Z.J. Li, Porous NiO nanofibers as an efficient electrocatalyst towards long cycling life rechargeable Li–CO<sub>2</sub> batteries, *Electrochim. Acta* 319 (2019) 958–965.
- [153] B. Liu, Y. Sun, L. Liu, S. Xu, X. Yan, Advances in manganese-based oxides cathodic electrocatalysts for Li–air batteries, *Adv. Funct. Mater.* 28 (2018) 1704973.
- [154] T.T. Truong, Y. Liu, Y. Ren, L. Trahey, Y. Sun, Morphological and crystalline evolution of nanostructured MnO<sub>2</sub> and its application in lithium–air batteries, *ACS Nano* 6 (2012) 8067–8077.
- [155] W. Ma, S. Lu, X. Lei, X. Liu, Y. Ding, Porous Mn<sub>2</sub>O<sub>3</sub> cathode for highly durable Li–CO<sub>2</sub> batteries, *J. Mater. Chem. A* 6 (2018) 20829–20835.
- [156] X. Lei, S. Lu, W. Ma, Z. Cao, R. Zhang, X. Liu, Y. Ding, Porous MnO as efficient catalyst towards the decomposition of Li<sub>2</sub>CO<sub>3</sub> in ambient Li–air batteries, *Electrochim. Acta* 280 (2018) 308–314.
- [157] Q. Liu, L. Geng, T. Yang, Y. Tang, P. Jia, Y. Li, H. Li, T. Shen, L. Zhang, J. Huang, In-situ imaging electrocatalysis in a Na–O<sub>2</sub> battery with Au-coated MnO<sub>2</sub> nanowires air cathode, *Energy Storage Mater.* 19 (2019) 48–55.
- [158] B. Ge, Y. Sun, J. Guo, X. Yan, C. Fernandez, Q. Peng, A co-doped MnO<sub>2</sub> catalyst for Li–CO<sub>2</sub> batteries with low overpotential and ultrahigh cyclability, *Small* 15 (2019) e1902220.
- [159] L. Mino, G. Spoto, A.M. Ferrari, CO<sub>2</sub> capture by TiO<sub>2</sub> Anatase surfaces: a combined DFT and FTIR study, *J. Phys. Chem. C* 118 (2014) 25016–25026.
- [160] G.K. Ramesha, J.F. Brennecke, P.V. Kamat, Origin of catalytic effect in the reduction of CO<sub>2</sub> at nanostructured TiO<sub>2</sub> films, *ACS Catal.* 4 (2014) 3249–3254.
- [161] J.M.T.A. Fischer, M. Hankel, D.J. Searles, Computational studies of the interaction of carbon dioxide with graphene-supported titanium dioxide, *J. Phys. Chem. C* 119 (2015) 29044–29051.
- [162] R. Pipes, A. Bhargav, A. Manthiram, Nanostructured Anatase titania as a cathode catalyst for Li–CO<sub>2</sub> batteries, *ACS Appl. Mater. Interfaces* 10 (2018) 37119–37124.
- [163] K. Oshikawa, M. Nagai, S. Omi, Characterization of molybdenum carbides for methane reforming by TPR, XRD, and XPS, *J. Phys. Chem. B* 105 (2001) 9124–9131.
- [164] N.M. Schweitzer, J.A. Schaidle, O.K. Ezekoye, X. Pan, S. Linic, L.T. Thompson, High activity carbide supported catalysts for water gas shift, *J. Am. Chem. Soc.* 133 (2011) 2378–2381.
- [165] C. Wan, Y.N. Regmi, B.M. Leonard, Multiple phases of molybdenum carbide as electrocatalysts for the hydrogen evolution reaction, *Angew. Chem. Int. Ed. Engl.* 53 (2014) 6407–6410.
- [166] H. Vrubel, X. Hu, Molybdenum boride and carbide catalyze hydrogen evolution in both acidic and basic solutions, *Angew. Chem. Int. Ed. Engl.* 51 (2012) 12703–12706.

- [167] M.D. Porosoff, X. Yang, J.A. Boscoboinik, J.G. Chen, Molybdenum carbide as alternative catalysts to precious metals for highly selective reduction of CO<sub>2</sub> to CO, *Angew. Chem. Int. Ed. Engl.* 53 (2014) 6705–6709.
- [168] W.J. Kwak, K.C. Lau, C.D. Shin, K. Amine, L.A. Curtiss, Y.K. Sun, A Mo<sub>2</sub>C/carbon nanotube composite cathode for lithium-oxygen batteries with high energy efficiency and long cycle life, *ACS Nano* 9 (2015) 4129–4137.
- [169] A. Hu, J. Long, C. Shu, R. Liang, J. Li, Three-dimensional interconnected network architecture with homogeneously dispersed carbon nanotubes and layered MoS<sub>2</sub> as a highly efficient cathode catalyst for lithium-oxygen battery, *ACS Appl. Mater. Interfaces* 10 (2018) 34077–34086.
- [170] M. Asadi, B. Sayahpour, P. Abbasi, A.T. Ngo, K. Karis, J.R. Jokisaari, C. Liu, B. Narayanan, M. Gerard, P. Yasaee, X. Hu, A. Mukherjee, K.C. Lau, R.S. Assary, F. Khalili-Araghi, R.F. Klie, L.A. Curtiss, A. Salehi-Khojin, A lithium-oxygen battery with a long cycle life in an air-like atmosphere, *Nature* 555 (2018) 502–506.
- [171] J. He, G. Hartmann, M. Lee, G.S. Hwang, Y. Chen, A. Manthiram, Freestanding 1T MoS<sub>2</sub>/graphene heterostructures as a highly efficient electrocatalyst for lithium polysulfides in Li-S batteries, *Energy Environ. Sci.* 12 (2019) 344–350.
- [172] R. Pipes, J. He, A. Bhargav, A. Manthiram, Efficient Li–CO<sub>2</sub> batteries with molybdenum disulfide nanosheets on carbon nanotubes as a catalyst, *ACS Appl. Energy Mater.* 2 (2019) 8685–8694.
- [173] H. Wang, K. Xie, Y. You, Q. Hou, K. Zhang, N. Li, W. Yu, K.P. Loh, C. Shen, B. Wei, Realizing interfacial electronic interaction within ZnS quantum dots/N-rGO heterostructures for efficient Li–CO<sub>2</sub> batteries, *Adv. Energy Mater.* 9 (2019) 1901806.
- [174] P. Lamagni, M. Miola, J. Catalano, M.S. Hvid, M.A.H. Mamakheh, M. Christensen, M.R. Madsen, H.S. Jeppesen, X.M. Hu, K. Daasbjerg, T. Skrydstrup, N. Lock, Restructuring metal-organic frameworks to nanoscale bismuth electrocatalysts for highly active and selective CO<sub>2</sub> reduction to formate, *Adv. Funct. Mater.* 30 (2020) 1910408.
- [175] L. Jiao, Y. Wang, H.L. Jiang, Q. Xu, Metal-organic frameworks as platforms for catalytic applications, *Adv. Mater.* 30 (2018) e1703663.
- [176] H. Deng, S. Grunder, K.E. Cordova, C. Valente, H. Furukawa, M. Hmadedh, F. Gandara, A.C. Whalley, Z. Liu, S. Asahina, H. Kazumori, M. O’Keffe, O. Terasaki, J.F. Stoddart, O.M. Yaghi, Large-pore apertures in a series of metal-organic frameworks, *Science* 336 (2012) 1018–1023.
- [177] H.C. Zhou, J.R. Long, O.M. Yaghi, Introduction to metal-organic frameworks, *Chem. Rev.* 112 (2012) 673–674.
- [178] K. Sumida, D.L. Rogow, J.A. Mason, T.M. McDonald, E.D. Bloch, Z.R. Herm, T.H. Bae, J.R. Long, Carbon dioxide capture in metal-organic frameworks, *Chem. Rev.* 112 (2012) 724–781.
- [179] S. Li, Y. Dong, J. Zhou, Y. Liu, J. Wang, X. Gao, Y. Han, P. Qi, B. Wang, Carbon dioxide in the cage: manganese metal-organic frameworks for high performance CO<sub>2</sub> electrodes in Li–CO<sub>2</sub> batteries, *Energy Environ. Sci.* 11 (2018) 1318–1325.
- [180] S. Kandambeth, K. Dey, R. Banerjee, Covalent organic frameworks: chemistry beyond the structure, *J. Am. Chem. Soc.* 141 (2019) 1807–1822.
- [181] N. Huang, P. Wang, D. Jiang, Covalent organic frameworks: a materials platform for structural and functional designs, *Nat. Rev. Mater.* 1 (2016).
- [182] C.S. Diercks, O.M. Yaghi, The atom, the molecule, and the covalent organic framework, *Science* (2017) 355.
- [183] A. Halder, M. Ghosh, M.A. Khayum, S. Bera, M. Addicoat, H.S. Sasmal, S. Karak, S. Kurungot, R. Banerjee, Interlayer hydrogen-bonded covalent organic frameworks as high-performance supercapacitors, *J. Am. Chem. Soc.* 140 (2018) 10941–10945.
- [184] E. Jin, J. Li, K. Geng, Q. Jiang, H. Xu, Q. Xu, D. Jiang, Designed synthesis of stable light-emitting two-dimensional sp(2) carbon-conjugated covalent organic frameworks, *Nat. Commun.* 9 (2018) 4143.
- [185] S. Yang, W. Hu, X. Zhang, P. He, B. Pattengale, C. Liu, M. Cendejas, I. Hermans, X. Zhang, J. Zhang, J. Huang, 2D covalent organic frameworks as intrinsic photocatalysts for visible light-driven CO<sub>2</sub> reduction, *J. Am. Chem. Soc.* 140 (2018) 14614–14618.
- [186] Q. Gao, X. Li, G.-H. Ning, H.-S. Xu, C. Liu, B. Tian, W. Tang, K.P. Loh, Covalent organic framework with frustrated bonding network for enhanced carbon dioxide storage, *Chem. Mater.* 30 (2018) 1762–1768.
- [187] S. Huang, D. Chen, C. Meng, S. Wang, S. Ren, D. Han, M. Xiao, L. Sun, Y. Meng, CO<sub>2</sub> nanoenrichment and nanoconfinement in cage of imine covalent organic frameworks for high-performance CO<sub>2</sub> cathodes in Li–CO<sub>2</sub> batteries, *Small* 15 (2019) e1904830.
- [188] X. Li, H. Wang, Z. Chen, H.S. Xu, W. Yu, C. Liu, X. Wang, K. Zhang, K. Xie, K.P. Loh, Covalent-organic-framework-based Li–CO batteries, *Adv. Mater.* 31 (2019) e1905879.
- [189] X. Zhang, Z. Wu, X. Zhang, L. Li, Y. Li, H. Xu, X. Li, X. Yu, Z. Zhang, Y. Liang, H. Wang, Highly selective and active CO<sub>2</sub> reduction electrocatalysts based on cobalt phthalocyanine/carbon nanotube hybrid structures, *Nat. Commun.* 8 (2017) 14675.
- [190] J. Chen, K. Zou, P. Ding, J. Deng, C. Zha, Y. Hu, X. Zhao, J. Wu, J. Fan, Y. Li, Conjugated cobalt polyphthalocyanine as the elastic and reprocessable catalyst for flexible Li–CO<sub>2</sub> batteries, *Adv. Mater.* 31 (2019) e1805484.
- [191] J.-Y. Lee, H.-S. Kim, J.-S. Lee, C.-J. Park, W.-H. Ryu, Blood protein as a sustainable bifunctional catalyst for reversible Li–CO<sub>2</sub> batteries, *ACS Sustainable Chem. Eng.* 7 (2019) 16151–16159.
- [192] X. Li, S. Yang, N. Feng, P. He, H. Zhou, Progress in research on Li–CO<sub>2</sub> batteries: Mechanism, catalyst and performance, *Chin. J. Catal.* 37 (2016) 1016–1024.
- [193] Z. Guo, J. Li, Y. Xia, C. Chen, F. Wang, A.G. Tamirat, Y. Wang, Y. Xia, L. Wang, S. Feng, A flexible polymer-based Li–air battery using a reduced graphene oxide/Li composite anode, *J. Mater. Chem. A* 6 (2018) 6022–6032.
- [194] W.-J. Kwak, D. Hirshberg, D. Sharon, M. Afri, A.A. Frimer, H.-G. Jung, D. Aurbach, Y.-K. Sun, Li–O<sub>2</sub> cells with LiBr as an electrolyte and a redox mediator, *Energy Environ. Sci.* 9 (2016) 2334–2345.
- [195] Z. Liang, Y.C. Lu, Critical role of redox mediator in suppressing charging instabilities of lithium-oxygen batteries, *J. Am. Chem. Soc.* 138 (2016) 7574–7583.
- [196] C. Zhao, J. Liang, X. Li, N. Holmes, C. Wang, J. Wang, F. Zhao, S. Li, Q. Sun, X. Yang, J. Liang, X. Lin, W. Li, R. Li, S. Zhao, H. Huang, L. Zhang, S. Lu, X. Sun, Halide-based solid-state electrolyte as an interfacial modifier for high performance solid-state Li–O<sub>2</sub> batteries, *Nano Energy* 75 (2020) 105036.
- [197] J.L. Ma, F.L. Meng, Y. Yu, D.P. Liu, J.M. Yan, Y. Zhang, X.B. Zhang, Q. Jiang, Prevention of dendrite growth and volume expansion to give high-performance aprotic bimetallic Li–Na alloy–O<sub>2</sub> batteries, *Nat. Chem.* 11 (2019) 64–70.
- [198] X.-G. Wang, C. Wang, Z. Xie, X. Zhang, Y. Chen, D. Wu, Z. Zhou, Improving electrochemical performances of rechargeable Li–CO<sub>2</sub> batteries with an electrolyte redox mediator, *ChemElectroChem* 4 (2017) 2145–2149.
- [199] T. Shiga, Y. Kato, M. Inoue, Y. Hase, Bifunctional catalytic activity of iodine species for lithium–carbon dioxide battery, *ACS Sustainable Chem. Eng.* 7 (2019) 14280–14287.
- [200] J.H. Rheinhardt, P. Singh, P. Tarakeshwar, D.A. Buttry, Electrochemical capture and release of carbon dioxide, *ACS Energy Lett.* 2 (2017) 454–461.
- [201] Y. Ding, Y. Li, G. Yu, Exploring bio-inspired quinone-based organic redox flow batteries: a combined experimental and computational study, *Chem* 1 (2016) 790–801.
- [202] W. Yin, A. Grimaud, I. Azcarate, C. Yang, J.-M. Tarascon, Electrochemical reduction of CO<sub>2</sub> mediated by quinone derivatives: implication for Li–CO<sub>2</sub> battery, *J. Phys. Chem. C* 122 (2018) 6546–6554.
- [203] A. Khurram, M. He, B.M. Gallant, Tailoring the discharge reaction in Li–CO<sub>2</sub> batteries through incorporation of CO<sub>2</sub> capture chemistry, *Joule* 2 (2018) 2649–2666.
- [204] R. Pipes, A. Bhargav, A. Manthiram, Phenyl disulfide additive for solution-mediated carbon dioxide utilization in Li–CO<sub>2</sub> batteries, *Adv. Energy Mater.* 9 (2019) 1900453.
- [205] A. Khurram, Y. Yin, L. Yan, L. Zhao, B.M. Gallant, Governing role of solvent on discharge activity in lithium–CO<sub>2</sub> batteries, *J. Phys. Chem. Lett.* 10 (2019) 6679–6687.
- [206] J. Yi, S. Guo, P. He, H. Zhou, Status and prospects of polymer electrolytes for solid-state Li–O<sub>2</sub> (air) batteries, *Energy Environ. Sci.* 10 (2017) 860–884.
- [207] K. Chen, G. Huang, J.L. Ma, J. Wang, D.Y. Yang, X.Y. Yang, Y. Yu, X.B. Zhang, The stabilization effect of CO<sub>2</sub> in lithium–oxygen/CO<sub>2</sub> batteries, *Angew. Chem. Int. Ed. Engl.* (2020).
- [208] C. Zhao, J. Liang, Q. Sun, J. Luo, Y. Liu, X. Lin, Y. Zhao, H. Yadegari, M.N. Banis, R. Li, H. Huang, L. Zhang, R. Yang, S. Lu, X. Sun, Ultralong-life quasi-solid-state Li–O<sub>2</sub> batteries enabled by coupling advanced air electrode design with Li metal anode protection, *Small Methods* 3 (2018) 1800437.
- [209] X. Lin, F. Sun, Q. Sun, S. Wang, J. Luo, C. Zhao, X. Yang, Y. Zhao, C. Wang, R. Li, X. Sun, O<sub>2</sub>/O<sub>2</sub> crossover and dendrite-free hybrid solid-state Na–O batteries, *Chem. Mater.* 31 (2019) 9024–9031.
- [210] C. Zhao, J. Liang, Y. Zhao, J. Luo, Q. Sun, Y. Liu, X. Lin, X. Yang, H. Huang, L. Zhang, S. Zhao, S. Lu, X. Sun, Engineering a “nanonet”-reinforced polymer electrolyte for long-life Li–O<sub>2</sub> batteries, *J. Mater. Chem. A* 7 (2019) 24947–24952.
- [211] J. Yi, X. Liu, S. Guo, K. Zhu, H. Xue, H. Zhou, Novel stable gel polymer electrolyte: toward a high safety and long life Li–air battery, *ACS Appl. Mater. Interfaces* 7 (2015) 23798–23804.
- [212] C. Li, Z. Guo, B. Yang, Y. Liu, Y. Wang, Y. Xia, A rechargeable Li–CO<sub>2</sub> battery with a gel polymer electrolyte, *Angew. Chem. Int. Ed. Engl.* 56 (2017) 9126–9130.
- [213] M. Mushtaq, X.-W. Guo, J.-P. Bi, Z.-X. Wang, H.-J. Yu, Polymer electrolyte with composite cathode for solid-state Li–CO<sub>2</sub> battery, *Rare Met.* 37 (2018) 520–526.
- [214] J. Shi, S. Peng, J. Pei, Y. Liang, F. Cheng, J. Chen, Quasi-solid-state dye-sensitized solar cells with polymer gel electrolyte and triphenylamine-based organic dyes, *ACS Appl. Mater. Interfaces* 1 (2009) 944–950.
- [215] Z. Zhu, M. Hong, D. Guo, J. Shi, Z. Tao, J. Chen, All-solid-state lithium organic battery with composite polymer electrolyte and pillar[5]quinone cathode, *J. Am. Chem. Soc.* 136 (2014) 16461–16464.
- [216] X. Hu, Z. Li, J. Chen, Flexible Li–CO<sub>2</sub> batteries with liquid-free electrolyte, *Angew. Chem. Int. Ed. Engl.* 56 (2017) 5785–5789.
- [217] R. Wang, X. Zhang, Y. Cai, Q. Nian, Z. Tao, J. Chen, Safety-reinforced rechargeable Li–CO<sub>2</sub> battery based on a composite solid state electrolyte, *Nano Res.* 12 (2019) 2543–2548.